Modeling and Route Guidance of Trucks in Metropolitan Areas

Principal Investigators:

Petros Ioannou

University of Southern California
Center for Advanced Transportation Technologies
EE-Systems, EEB200, MC2562
Los Angeles, CA. 90274

Anastasios Chassiakos

California State University
College of Engineering
Long Beach, CA. 90840-5602

Research Associates and Graduate Students:

Arnab Bose
Hossein Jula
Alex Kanaris
Hamid Pourmohammadi
Jose Sotelo
Katarina Vukadinovic
Ricardo Unglaub

August 2000
Revised February 12, 2001

METRANS Transportation Center
USC CSULB

Disclaimer

The contents of this report reflect the views of the authors, who are responsible for the facts and the accuracy of the information presented herein. This document is disseminated under the sponsorship of the Department of Transportation, University Transportation Centers Program, and California Department of Transportation in the interest of information exchange. The U.S. Government and California Department of Transportation assume no liability for the contents or use thereof. The contents do not necessarily reflect the official views or policies of the State of California or the Department of Transportation. This report does not constitute a standard, specification, or regulation.

Abstract

The efficient movement of goods in a metropolitan area, where congestion on highways and surface streets is part of daily life, has become more and more challenging. In this project, we analyze the effect of trucks on traffic flow, and consider methods for routing trucks through a complex transportation network. Our results are presented in parts I and II of the report. In part I, using truck and driver models, we have shown that the slower dynamical response of trucks relative to that of passenger vehicles leads to lower traffic flow rates and influence the traffic flow characteristics in various ways that are analyzed. The analytical results compare well with those based on empirical studies presented in the Highway Capacity Manual. The dynamical characteristics of trucks are taken into account in part II in order to develop routing algorithms for trucks in a transportation network that involves highways and surface streets. We assume that traffic information is available on-line so that uncertainties due to variations in traffic conditions are eliminated or significantly reduced. Applying some of today's sensor and information technologies can satisfy this assumption. We use deterministic dynamic routing techniques to route trucks through a complex transportation network in order to minimize travel time. The routing algorithms are simulated using a traffic network from the Los Angeles metropolitan area. We have demonstrated that dynamic routing could reduce travel time significantly. A reduction in travel time could translate into considerable savings and to a more efficient movement of goods.

Table of contents

List of Tables

List of Figures

Disclosure

Project was funded in entirety under this contract to California Department of Transportation.

Acknowledgments

The authors would like to thank Ms. Susan Bok and Steve Mermelstein and their group of the department of transportation of the city of Los Angeles for numerous discussions and suggestions regarding truck traffic and routing in the city of Los Angeles.

Part I: EFFECT OF TRUCK DYNAMICS ON TRAFFIC FLOW

1 INTRODUCTION

Heavy-duty commercial vehicles form an important facet of the transportation industry. They transport goods that we use daily and thus influence our lives in many ways. It is commonly believed that heavy-duty trucks have a detrimental impact on traffic flow rates. Their longer length, low actuation-to-weight ratio and slower dynamical response compared to passenger vehicles may cause traffic disturbances leading to the generation of shock waves, traffic delays, adverse variations in vehicle speeds, etc. In addition, their huge size and inertia pose safety concerns in case of accidents and may influence the response of the drivers of passenger vehicles. The impact is more pronounced on grades and curves that necessitate special right-of-the-way rules and imposes constraints on highway designs. The nature and the degree of the effect of trucks on traffic flow need to be understood and quantified in order to find better ways to deal with truck traffic and truck routing especially in metropolitan areas where the need for highway capacity is increasing and congestion is becoming a crucial problem. The scope of Part I of this report is to focus on the analysis and impact of truck dynamics on traffic flow, both on the microscopic and macroscopic level.

On the microscopic level mathematical models are used to assess the response of vehicles and trucks operating in a mixed passenger car/truck traffic. The response of passenger vehicles is modeled using a human driver car following model, namely the Pipes' model [Pipes, 1953; Chandler, 1958]. This model is chosen among the several available models in transportation literature because it has been demonstrated that it models the response of passenger vehicles during transients in traffic flow [Bose and Ioannou, 2000] more accurately than other models. On the other hand, a high fidelity truck model is used that describes the dynamical response of heavy-duty trucks in vehicle following scenarios.

The slower dynamics, low weight-to-actuation ratio and lower deceleration of the trucks in comparison to the average passenger car affect the stopping distance. In other words, trucks require a larger distance to come to a complete stop from a given speed than passenger cars. As a result, a truck should follow another vehicle in traffic flow at a greater distance than a passenger car in order to avoid a collision when the lead vehicle performs deceleration maneuvers. This translates into larger inter-vehicle spacing requirements for trucks in order to reduce the possibility of rear-end collisions. High inter-vehicle spacing, however, has a negative effect on capacity. While in practice drivers may violate minimum safety inter-vehicle spacing, it is postulated that on the average truck drivers maintain an inter-vehicle spacing that takes into account their reaction time and truck dynamical characteristics. In part I of this report, we examine the effect of truck dynamics on inter-vehicle spacing and on capacity as a function of the percentage of trucks in a mixed traffic involving passenger vehicles. We show that the higher inter-vehicle spacing required by trucks reduces capacity as the percentage of

trucks mixed with passenger vehicles increases. Our analytical results compare well with empirical data in the Highway Capacity Manual.

The different dynamical characteristics of trucks are expected to affect transients in traffic flow. We use a microscopic analysis to investigate the vehicle-to-vehicle interaction in mixed truck/passenger car traffic and compare it with 100% passenger car traffic. We observe that the slow dynamics and limited acceleration of the trucks create a large inter-vehicle spacing when the truck cannot keep up with the accelerating passenger cars. The slowly accelerating truck retards the response of the following vehicles. We demonstrate that a truck filters the fast acceleration transients generated by passenger cars and converts it to a smoother velocity response that can be easily tracked by another following truck. We also demonstrate that the total travel time of a vehicle in mixed truck/passenger car traffic increases in comparison to the total travel time over the same time horizon in 100% passenger traffic.

On the macroscopic level the variables of interest are traffic flow and density, vehicular speed averaged over intervals of time and space. In this case the focus is on the response characteristics of the traffic flow rather than the response of individual vehicles. We show in a graphical way that the presence of trucks slows the upstream propagation of shock waves in traffic flow due to their slower reaction time. This reaction time is the sum of the driver reaction time and the actuator delays. Shock waves are discontinuous traffic flow waves that occur when traffic on a section of a road is denser in front and less dense behind. Furthermore, we show graphically that trucks in mixed truck/passenger car traffic reduce average traffic density and traffic flow rate. Simulations are used to demonstrate our theoretical findings. We use a simplified linear model of the truck longitudinal model presented in Section 2 and assume 10% truck penetration in mixed truck/passenger car traffic. In our simulations, we demonstrate that a shock wave travels upstream faster in 100% passenger car traffic than in mixed truck/passenger car traffic. Furthermore, we observe that the average traffic speed increase due to the shock wave is retarded by the slow acceleration of the trucks in mixed truck/passenger car traffic.

The part I of the report is organized as follows: in Section 2 we present the longitudinal and lateral truck models used in our analysis. In Section 3 we analyze the inter-vehicle spacing requirements of truck and the effect of trucks on highway capacity. In Section 4 we present the microscopic analysis and in Section 5 we present the macroscopic analysis of mixed truck/passenger car traffic.

2 TRUCK MODEL

In this section, we briefly outline the longitudinal and lateral truck models used in our analysis. The truck configurations used are similar to those of the tractor semi-trailer truck. The truck model is used to describe the dynamical response of heavy-duty trucks in traffic flow vehicle following scenarios and during lane changes.

2.1 Longitudinal Model

The longitudinal model is used to represent the dynamical response of a truck in the longitudinal direction. The change in the linear momentum is given by the difference of the active tractive and passive resistance dissipative forces i.e.

$$\frac{d}{dt}MV = F_{traction} - F_{grade} - F_{aero} - F_{rolling} \quad (1)$$

where, M is the mass of the truck, V is the velocity of the truck, $F_{traction}$ is either the net braking force (negative sign) or the net propulsive force generated by the truck engine (positive sign) acting on the wheels, F_{grade} is the force required to travel a graded road, F_{aero} is the aerodynamic resistance and $F_{rolling}$ is the rolling resistance.

The force constitutive relations in (1) are defined as follows:

- Active Tractive Forces:
  The $F_{traction}$ term is the net active force either related to the engine torque through the throttle action or to the braking torque generated on the wheels by the braking system. It should be noted that a fraction of the active force is used either to accelerate or decelerate the rotating masses of the engine, transmission, wheels and axles. In the longitudinal model, the acceleration or deceleration of the rotating masses is considered by using an equivalent moment of inertia, J_{equiv} and the inertial force, $F_{inertia}$ corresponding to the rotating masses. The rotating inertia force, $F_{inertia}$, can be obtained from the following equations:

  $$\frac{d}{dt}J_{equiv} \cdot w = T_{inertia} \quad (2)$$

  $$T_{inertia} = F_{inertia} \cdot R_w \quad (3)$$

  $$V = w \cdot R_w \quad (4)$$

  leading to the equation:

  $$F_{inertia} = \frac{d}{dt}J_{equiv}R_w^{-2}V \quad (5)$$

where, $T_{inertia}$ is the inertia torque, $F_{inertia}$ is the inertia force, w is the wheel angular velocity, R_w is the wheel radius and J_{equiv} is the equivalent lumped mass moment of inertia reflected to the wheel axis.

Engine variables such as torque, T_{eng} and angular velocity, w_{eng} can be expressed in terms of the wheel rotating axis variables as follows:

$$J_{eng} = r^{-2} \cdot J_{wheel} \tag{6}$$

$$T_{eng} = r^{-1} \cdot T_{wheel} \tag{7}$$

$$w_{eng} = r \cdot w \tag{8}$$

where, r is the total rotation ratio from the engine axis to the wheel axis (called gear ratio in the model), and $r>1$ for road vehicles. W_{eng} is the engine rpm; J_{wheel} is the moment of inertia of rotating masses with respect to the wheel axis; T_{eng} is the engine torque; T_{wheel} is the torque at the wheels, and J_{eng} is the moment of inertia of rotating masses with respect to the engine axis.

By adding equation (5) to both sides of (1) we end up with the following modified linear momentum equation:

$$\frac{d}{dt}\left[\left(M + J_{equiv} R_w^{-2}\right) V\right] = \left(F_{traction} + F_{inertia}\right) - F_{grade} - F_{aero} - F_{rolling} \tag{9}$$

We notice that in (9) an additional inertia term adds to the truck mass. The term $(F_{traction} + F_{inertia})$ is easily identified as the total available active force (source) either from the engine F_{eng} (positive sign) or from the brakes F_{brake} (negative sign), given by (11) and (12) respectively.

The engine active force is directly related to the engine torque by using (7) and dividing by R_w similarly as in (3).

The engine torque, T_{eng} and rpm w_{eng} are related through the engine characteristic curves that are obtained through dynamometric tests. The curves are parameterized by the degree of throttle opening. The model assumes a proportional relation between the motor torque at full and partial throttling.

In the model T_{eng} is assumed to be expressed by a quadratic function with respect to the engine speed, as follows:

$$T_{eng} = C w_{eng}^2 + B w_{eng} + A \tag{10}$$

where, C,B and A are constants determined from engine data.

The tractive force F_{eng} is now obtained from the equation below:

$$F_{eng} = \delta.T_{eng}\left(r.R_w\right)^{-1} \quad , \; 1 \geq \delta \geq 0 \tag{11}$$

where δ is a constant accounting for the throttle opening.

The braking force is derived from the braking torque, which acts directly on the wheel axis. A simplified model for braking is derived by assuming that the adhesion coefficient is large enough to avoid sliding of the tires on the pavement and a maximum braking torque T_{brkmax} can be applied to the truck wheels resulting in a maximum deceleration value of 0.3g for emergency braking. The actual braking torque T_{brake} applied to decelerate the truck in service is assumed to be proportionally related to T_{brkmax}. The brake active force is obtained from:

$$F_{brake} = -k.T_{brk\max}.R_w^{-1} \quad , \qquad \text{with} \quad 1 \geq k \geq 0 \tag{12}$$

A switching logic is incorporated in the model to cut off the engine power when a braking action is necessary. The function S(t) defined in Table 1 helps to define analytically the tractive forces used in this model.

Finally, by using the switching function S(t) the $F_{traction}$ force in the linear momentum equation (1) can be easily be deduced from the first right-hand side term in parenthesis of equation (9) and by using equation (5) leading to:

$$F_{traction} = S(t).F_{eng} + (1(t) - S(t))F_{brake} - R_w^{-2}\frac{d}{dt}J_{equiv}V \tag{13}$$

1(t) in the above equation is the Heaviside function. It is 0 for t less than zero and 1 for t equal or greater than zero.

- Force required to travel a graded road:

$$F_{grade} = Mg \cdot \theta \tag{14}$$

where, Mg is the vehicle weight and θ is the grade slope (%).

- Aerodynamic Resistance:

$$F_{aero} = 0.5\rho \cdot V^2 \cdot C_d \cdot A_F \tag{15}$$

where, ρ is the air density, C_d is the aerodynamic drag coefficient, and A_F is the vehicle frontal projected area.

- Rolling Resistance:

$$F_{rolling} = (a + b \cdot V) \cdot Mg.C_r \tag{16}$$

where, a and b are constant parameters and C_r is a parameter that stands for the pavement condition (i.e., C_r=*1.0* for good pavement condition).

The equations of the truck model explained above are in Table 1.

Table 1: Summary of the Longitudinal Dynamic Model

Component Model	Equations(*)
Longitudinal Model .(Modified Linear Momentum equation.)	$\frac{d}{dt}\left[\left(M + J_{equiv} R_w^{-2}\right) V\right] = \left(F_{traction} + F_{inertia}\right) - F_{grade} - F_{aero} - F_{rolling}$
Rotating Inertia Force	$F_{inertia} = \frac{d}{dt} J_{equiv} R_w^{-2} V$
Net Tractive Forces	$F_{traction} = S(t).F_{eng} + [1(t) - S(t)].F_{brake} - F_{inertia}$
Engine Force and Torque	$F_{eng} = \delta.T_{eng}\left(r.R_w\right)^{-1}$ $T_{eng} = Cw_{eng}^2 + Bw_{eng} + A$
Brake Force	$F_{brake} = -k.T_{brk\max}.R_w^{-1}$
Grade Force	$F_{grade} = Mg \cdot \theta$
Aerodynamic Resistance	$F_{aero} = 0.5\rho \cdot V^2 \cdot C_d \cdot A_F$
Rolling Resistance	$F_{rolling} = (a + b \cdot V) \cdot Mg.C_r$
(*) For explanation of abbreviations refer to page 7	

The abbreviations used in Table 1 are as follows:

M: the mass of the truck
V: the velocity of the truck
r : the total rotation ratio from the engine axis to the wheel axis (called gear ratio) $r>1$ for road vehicles
w: the wheel angular velocity
ρ : the air density
θ : the grade slope (%)
k : the variable accounting for the amount of brake force applied to the vehicle
δ : the variable accounting for the throttle opening
A,B,C : constants determined from engine data
a,b : constant rolling coefficient parameters
A_F: the vehicle frontal projected area
C_d: the aerodynamic drag coefficient
C_r: a parameter that stands for the pavement condition (i.e., $C_r=1.0$ for good pavement condition)
R_w: the wheel radius
F_{aero}: the aerodynamic resistance
F_{grade} : the force required to travel a graded road
$F_{rolling}$: the rolling resistance
$F_{inertia}$: the rotating inertia force
$F_{traction}$: either the net braking force (negative sign) or the net propulsive force generated by the truck engine (positive sign) acting on the wheels
F_{eng}: the total available active force from the engine
F_{brake}: the total available active force from the brakes
J_{equiv}: the equivalent lumped mass moment of inertia reflected to the wheel axis
T_{brkmax}: maximum braking torque
T_{eng}: engine torque
w_{eng}: the engine speed
l(t): the Heaviside function, 0 for t less than zero and 1 for t equal or greater than zero
S(t): the switching function S(t)=0 if brake is applied
S(t)=1 otherwise

The parameter values used in the model for analysis and simulations are given in Table 2.

Table 2: Longitudinal truck model parameter values

PARAMETERS	VALUES
Truck Mass (M)	40,000 kg
Truck Frontal Projected Area (A)	10 m^2
Aerodynamic Drag Coefficient (C_d)	0.9
Wheel Radius (R_w)	0.5 m
Air Density (ρ)	1.0 $Nm^{-4}s^2$
Rolling Coefficients: a, b, C_r	0.012, 2.858e-04, 1.0
Engine Data (A, B, C)	-4067, 77.1, -0.25
Moment of Inertia (J_{equev})	5.96e03 Nm/s
Maximum Braking Torque (T_{brkmax})	50000 Nm
Nominal Engine Power	400 HP

The specific parameter values given in Table 2 correspond to a truck able to generate a maximum acceleration of 0.03g and a maximum deceleration of 0.3g. We will use these values for the rest of this report. It is worth mentioning that the maximum braking capability of the truck depends on its configuration (i.e. number of trailers) and can go up to 0.45g [Francher, 1997]. For safety and comfort the normal braking deceleration is kept well below the maximum possible used for emergencies.

2.2 Lateral Model

A kinematical model based on a realistic lateral acceleration profile is used to model the lateral motion of a truck as it performs a lane changing/merging maneuver. In the lane changing/merging maneuver a truck changes its lateral position to depart from its current lane and join the traffic in the adjacent lane.

In our analysis, we assume a simple but realistic model for the lateral acceleration, $a_{lat}(t)$ for a truck performing lateral displacement [Shladover, 1991] and is given as follows:

$$a_{lat}(t) = \begin{cases} \frac{2\pi H}{t_{lat}^2} \times \sin(\frac{2\pi}{t_{lat}}(t - t_{adj})) & t_{adj} \le t \le t_{lat} + t_{adj} \\ 0 & \textit{Otherwise} \end{cases} \qquad (17)$$

In the above equation, H is the total lateral displacement, t_{adj} is the time elapsed before lateral acceleration applies, and t_{lat} is the time after t_{adj} needed to complete the lateral displacement. It should be noted that the lateral acceleration $a_{lat}(t)$ according to (17), is positive within the first half of the lateral displacement, i.e. $t<(t_{lat}/2)+t_{adj}$, and negative in the second half.

Given the lateral velocity $v_{lat}(t)$, and lateral position $y_{lat}(t)$, $a_{lat}(t)$ can be easily computed by successive integration. In section 3.2, this lateral model is used to determine the safe and unsafe regions for a truck merging into the traffic in the adjacent lane. The model is

used to analyze the performance of the truck in a two-lane highway. The methodology can be easily extended and used for multi-lane highway as well.

It should be noted that the standard lane width on highways is 12 feet (3.68 meters) and this value is used as the total lateral displacement, H, in our analysis. The value of t_{adj} depends on the truck's initial relative spacing and velocity and it is the time taken by the driver to create enough spacing and to adjust the longitudinal velocity before starting lateral displacement. In our analysis, we assume this value to be zero.

Considering a highway with a fixed lane width H, the aggressiveness of lane changing maneuver depends primarily on the value of t_{lat}. Assuming a value for t_{lat}, the peak lateral acceleration $A = \max_t \{a_{lat}(t)\}$ can be determined based on (17). For a typical truck, the maximum peak of the lateral acceleration A cannot exceed 0.3g as it leads to truck instability and truck turn over. This value corresponds to t_{lat}=2.8 seconds. On the other hand, lane changes up to 16 seconds are not outside the normal range [Enke, 1979]. One can easily see that the total lane changing time t_{lat} may vary widely. In this report, we use a value of $t_{lat}=8$ seconds which results to a peak lateral acceleration $A=0.037g$.

3 SAFETY SPACING AND CAPACITY

3.1 Safe Spacing for Vehicle Following

Rear-end collisions in vehicle following in a single lane can occur during vehicle maneuvers if the spacing separating the vehicles is not large enough relative to the type of the maneuver, vehicle characteristics, driver reaction times, condition of the road, etc. In [Kanaris et al., 1996] a worst case scenario is assumed in order to find the minimum inter-vehicle spacing for avoiding rear-end collisions. The scenario assumes that the lead vehicle performs an emergency stopping maneuver using the maximum possible deceleration and the following vehicle responds after a certain delay with a particular deceleration response. The analysis in [Kanaris et al., 1996] focuses on vehicles of the same class, namely passenger vehicles. When different classes of vehicles are mixed the minimum spacing requirements change due to the differences in dynamic characteristics.

In this section, we assume that the trucks operate in the same lane as passenger vehicles and calculate the minimum initial spacing requirement for safe vehicle following. These spacing requirements are then used to calculate possible capacity estimates in mixed traffic involving passenger vehicles and trucks.

Fig.1 shows the worst-case scenario assumed for safe spacing calculation.

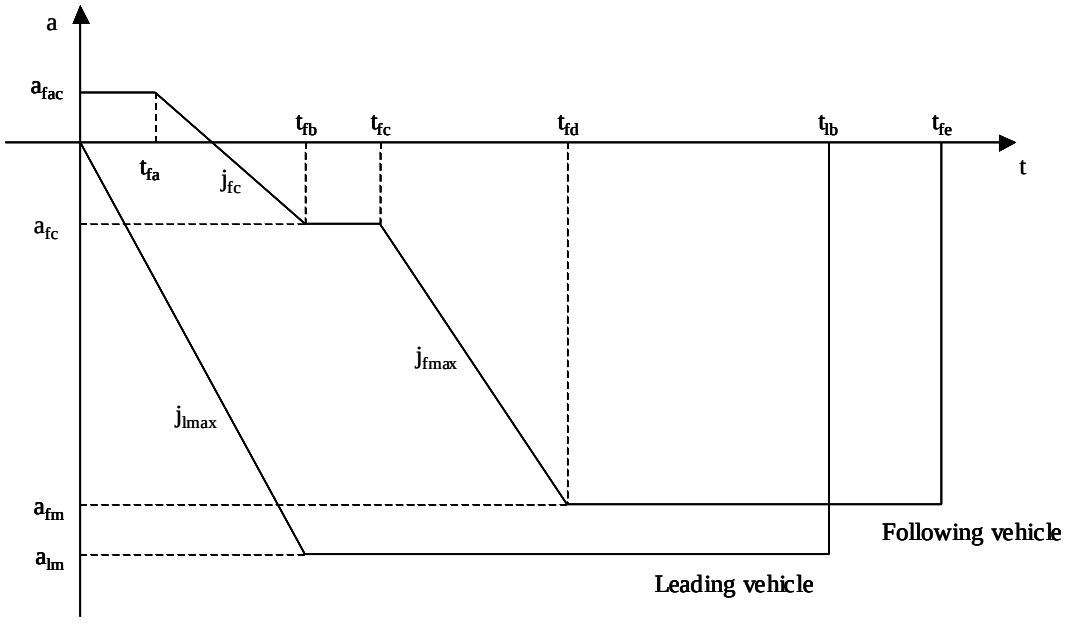

Fig. 1: Acceleration profiles during assumed worst-case stopping scenario

The leading vehicle performs emergency braking at time *t=0*, at a maximum rate of change (jerk) equal to j_{lmax} until it reaches a maximum possible deceleration of a_{lm}. The follower, which might have been accelerating initially at a_{fac} starts decelerating after a detection and brake actuation delay equal to t_{fa} in an effort to maintain the desired spacing. Since initially the follower is not aware that the leader is performing emergency

braking, it limits its jerk and deceleration to j_{fc} and a_{fc} respectively, in an effort to maintain smooth driving. At time $t=t_{fc}$ the follower detects that the leading vehicle is performing an emergency stopping maneuver in which case the driver performs braking with maximum jerk j_{fmax} and maximum possible deceleration a_{fm}.

In this section, we use the above stopping scenario to calculate the minimum initial spacing between vehicles for collision free vehicle following by substituting appropriate numerical values for the various parameters.

In evaluating the above scenario, we adopted a set of likely initial conditions at the onset of braking. The assumptions regarding the initial conditions are as follows. The leader is assumed to be a passenger car that is traveling at different speeds 10, 30, 50, and 70 miles per hour. The follower is assumed to be a truck (tractor, semi-trailer) having an initial velocity varying from 10 to 80 mph and zero initial acceleration, i. e. $a_{fac}=0$. These conditions represent realistic scenarios. We assumed a 1.0 second delay for detection and a 0.7 seconds delay for the actuator. When the vehicle detects that the leader is braking, the follower applies limited braking at first, with the objective of precaution and preparation for further actions. The jerk is limited to 5 meters/sec^3 during this phase, till its deceleration reaches the normal deceleration $a_{fc} = -0.1\ g$. In other words, the vehicle initially applies a limited amount of braking because at the onset of braking it is not known if the leader is simply slowing down or performing emergency braking. Eventually, the follower detects that the headway is diminishing rapidly and therefore concludes that the leader is performing emergency braking maneuver. We assumed that the human detection and actuator delay for emergency braking is 0.8 seconds, which is in addition to the initial delay of 1.7 seconds, that is in Fig. 1 the value of t_{fc} is assumed to be 1.7+0.8=2.5 seconds. The follower keeps braking until it reaches the maximum allowable deceleration $a_{fm}=-0.3\ g$.

The simulation software SPACING [Ioannou, 1996] is used to determine the safe and unsafe regions in a rear-end vehicle following scenario. Tables 3 and 4 show the values adopted for the scenario. The 'safe' and the 'unsafe' regions are shown in Fig. 2 for different leading vehicle's initial velocity.

Table 3: Braking parameters for the following vehicle

Following Vehicle (Truck)	
Initial Velocity	10 – 80 mph
Initial Acceleration	0
Detection plus Actuation Delay	1.7 sec
Normal Jerk	5 m/s^3
Emergency Deceleration	0.3 g
Friction Coefficient	1
Normal Deceleration	0.1 g
Emergency Delay	2.5 sec
Emergency Jerk	30 m/s^3

Table 4: Braking parameters for the leading vehicle

Leading Vehicle (passenger car)	
Initial Velocity	10 - 70 mph
Friction Coefficient	1
Emergency Deceleration	0.8 g
Emergency Jerk	50 m/s^3

Each curve in Fig. 2 divides the initial spacing–truck velocity plane into two regions: 'safe' and 'unsafe'. The unsafe region shrinks as the leading vehicle's initial velocity increases. Furthermore, as truck initial velocity increases the initial spacing to avoid collision increases, as well.

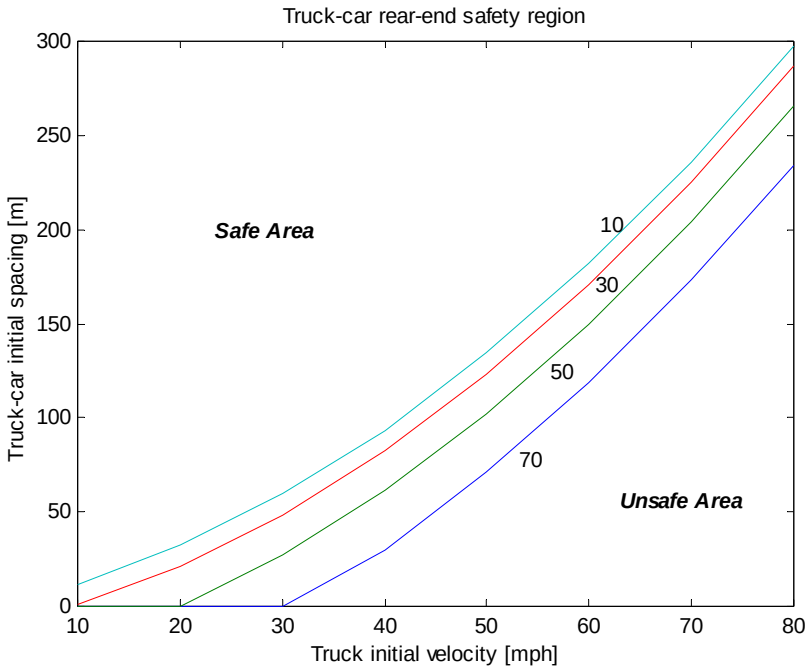

Fig. 2: Safe and unsafe regions for truck-car following in the same lane. The curves are parameterized by the leading passenger car initial velocity.

As shown in Fig. 2, for truck (following) and passenger car (leading) vehicles' velocities equal to 60 and 50 mph, respectively, the initial safety spacing is approximately 150 meters. This value indeed is the ideal lower bound derived from kinematical considerations. Other safety considerations have their own effects on increasing the initial safety spacing for no rear-end collision scenario. To name a few, one may consider the effect of truck configurations, stability constraint, and tire-pavement adhesion conditions. The effects are mainly due to the limitations applied on the maximum deceleration allowed during the braking maneuver.

The effect of maximum emergency deceleration on initial minimum safety spacing is elaborated more in Fig. 3. Let's assume that the maximum emergency deceleration a_{fm}=*-0.3* is the baseline value for the sensitivity analysis. We apply up to ±33% deviation

to the baseline value. That is we are considering the braking scenarios where the maximum emergency deceleration can vary between –0.2g to –0.4g. We also assume that the leading and following vehicles are traveling with the initial velocities equal to 50 and 60 miles per hour, respectively. Fig. 3 shows the sensitivity of the safe and unsafe regions to the variations of the maximum emergency deceleration.

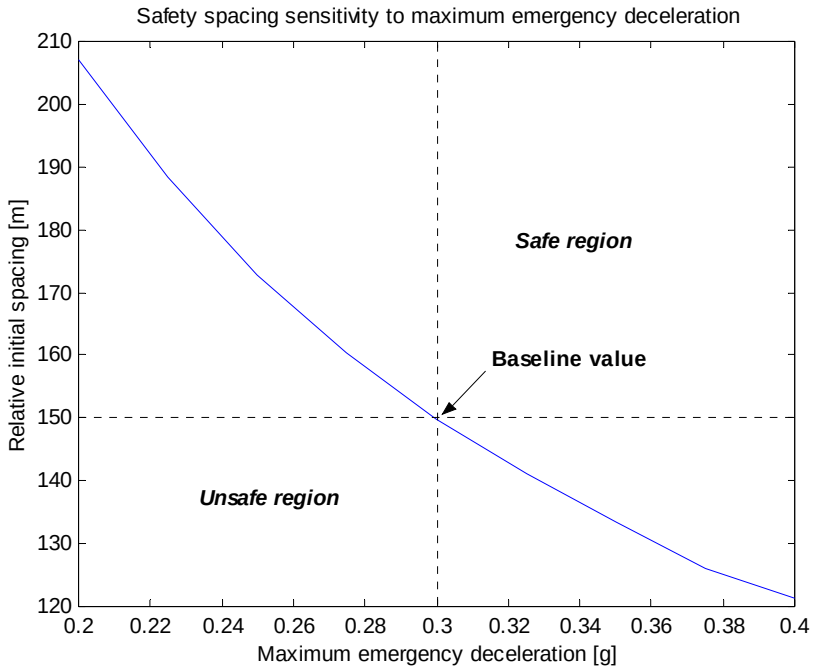

Fig. 3: Variation in minimum initial safety spacing with regard to maximum emergency deceleration.

3.2 Capacity Estimates

According to [Kanaris et al., 1996], the maximum possible highway throughput referred to as the capacity *C*, measured as the number of vehicles per hour per lane, is given by the following formula:

$$C = 3.6\times10^5 V \times \left[(100 - 2W_T)(L_P + h_{PP}V) + W_T(L_P + h_{PT}V + h_{TP}V + L_T)\right]^{-1} \quad (18)$$

where V is the speed of flow measured in meters/sec, Lp is the length of passenger cars, and L_T is the length of trucks with trailers, in meters. The parameter h_{PP} is the minimum headway in seconds between passenger cars; h_{PT} is the minimum headway in seconds between a passenger car and a truck that follows it; h_{TP} is the minimum headway in seconds between a truck and a passenger car that follows it, in seconds and W_T is the percentage of trucks in the mixed passenger car/truck traffic.

Equation 18 assumes that a truck is always positioned between two passenger vehicles and the passenger vehicle recognizes and uses the fact that the truck can decelerate much

slower that a passenger vehicle. Alternatively we consider the case when the passenger vehicle assumes that the truck in front has the same deceleration capabilities as a passenger vehicle. In this case instead of (18) we use the following equation for the capacity.

$$C = 3.6\times10^5 V \times\left[(100-2W_T)(L_P + h_{PP}V) + W_T\left(L_P + h_{PT}V + h_{PP}V + L_T\right)\right]^{-1} \quad (19)$$

Table 5 presents the numerical values necessary to define the braking deceleration profiles and the corresponding headway in a typical highway. *PP* stands for passenger car leader and passenger car follower; *PT* passenger car leader and truck follower, *TP* truck leader and passenger car follower, and finally *TT* truck leader and truck follower.

Table 5: The variable used to determine the capacity of a typical highway

		PP	**PT**	**TP**	**TT**
V_{l0}	mph	60	60	60	60
V_{f0}	mph	63	63	63	63
a_{lmax}	g	.8	0.8	0.3	0.3
a_{fmax}	g	.72	0.27	0.72	0.27
J_{lmax}	m/s^3	50	50	30	30
J_{fmax}	m/s^3	50	30	50	30
μ_{lmax}		1	1	1	1
μ_{fmax}		1	1	1	1
a_{fc}	G	0.2	0.1	0.2	0.1
a_{fac}	G	0.1	0.03	0.1	0.03
J_{fc}	m/s^3	8	5	8	5
t_{fa}	Sec	1.2	1.7	1.2	1.7
t_{fc}	Sec	1.8	2.5	1.8	2.5
Min headway	Sec	2.25	6.11	0.52	3.42
Min headway	Meters	63.46	172.03	14.69	96.42

Using the headway values presented in Table 5 and assuming that the speed of the flow is *V = 60* mph, then from (18) we have that the capacity of the highway is 1500 passenger cars per hour per lane. Table 6 column 2 presents the loss in the highway capacity for different road conditions and different percentage of trucks on the road. The results are calculated based on equation (18). Four different situations are considered in Table 6. Initially, we assume that there are no trucks in the traffic stream, i.e. 100% passenger car traffic (W_T*=0%*). The 100% passenger car traffic is assumed to be the baseline. Then different percentages of penetration of trucks in mixed truck/passenger car traffic are considered. That is we evaluate the highway capacity loss for W_T*=2.5%*, W_T*=5%*, and W_T*=10%* compared to the baseline.

In another approach which is considered in Table 6 (columns 2 and 3) and is presented in the Highway Capacity Manual (1998), the freeway capacity is defined as the maximum sustained 15-min rate of flow, expressed in passenger cars per hour per lane (pcphpl), that can be accommodated by a uniform freeway segment under prevailing traffic and roadway conditions in a specified direction. According to the Highway Capacity Manual

and in order to estimate the effect of the heavy vehicles on the freeway flow, each heavy vehicle is converted (adjusted) into equivalent number of passenger cars. The heavy traffic adjustment factor f_{HV} is defined as follows.

$$f_{HV} = \frac{1}{1 + P_T(E_T - 1) + P_R(E_R - 1)}$$

where

E_T = passenger-car equivalent for trucks and busses,
E_R = passenger-car equivalent for Recreational Vehicles (RVs),
P_T = proportion of trucks and busses in the traffic stream, and
P_R = proportion of RVs in the traffic stream.

Given E_T, E_R, P_T, P_R the factor f_{HV} can be calculated. The capacity then is equal to the product of the factor f_{HV} and the assumed base line capacity of 1500 cars per lane per hour Let's assume that there are no RVs traveling on the freeway, i.e. $P_R = 0$ and that the terrain of the freeway is level. Looking into the Passenger-Car Equivalent Tables for trucks and buses provided in the Highway Capacity Manual the value of E_T is found to be equal to *1.5*. Table 6 shows the losses in the highway capacity for $E_T = 1.5$ and $E_T = 2$ and for different percentage of truck penetration in the mixed traffic and compares the empirical results of the Highway Capacity Manual (1998) with our analysis results.

Table 6: Highway capacity changes due to trucks

Truck percentage in the mixed traffic	Changes in the capacity based on analysis using Eq.(18)	Changes in the capacity based on empirical results presented in Highway capacity Manual (1998)	
		E_T=2	E_T=1.5
	% Change	% Change	% Change
0% (Base line)	0	0	0
2.5%	-2.7	-2.5	-1.3
5%	-5.3	-4.8	-2.5
10%	-9.9	-9.1	-4.8

The results of the quantitative analysis in Table 6 (columns 2) indicate that the capacity of the lane decreases as the truck percentage in the mixed traffic increases. It should be noted that the percentage decrease in capacity is proportional to the percentage increase of the number of trucks in mixed traffic.

The empirical results from Highway Capacity Manual are in very close agreement with our analysis results for the case of $E_T = 2$. Our analysis was based on the assumption that the minimum safety spacing calculated are followed by all drivers of the trucks and passengers vehicles. Even though this is an ideal situation, our results may suggest that on the average drivers do maintain spacings that are close to the safe ones calculate in this report.

3.3 Effects of Trucks on Traffic Flow Characteristics

In the previous section, and in order to estimate the effect of the heavy vehicles on the traffic characteristics, each heavy vehicle was converted into its equivalent number of passenger cars using the heavy vehicle adjustment factor, f_{HV}. Similarly, the equivalent passenger car density[1] for the mixed traffic can be defined and calculated using the adjustment factor, f_{HV}. Having the equivalent passenger car density, one can use the fundamental equation describing the traffic stream[2] to evaluate the impact of the presence of heavy vehicles on the traffic flow characteristics.

Figure 4 shows the relation between the traffic flow rate Q, and density D of a traffic stream in a typical highway system.

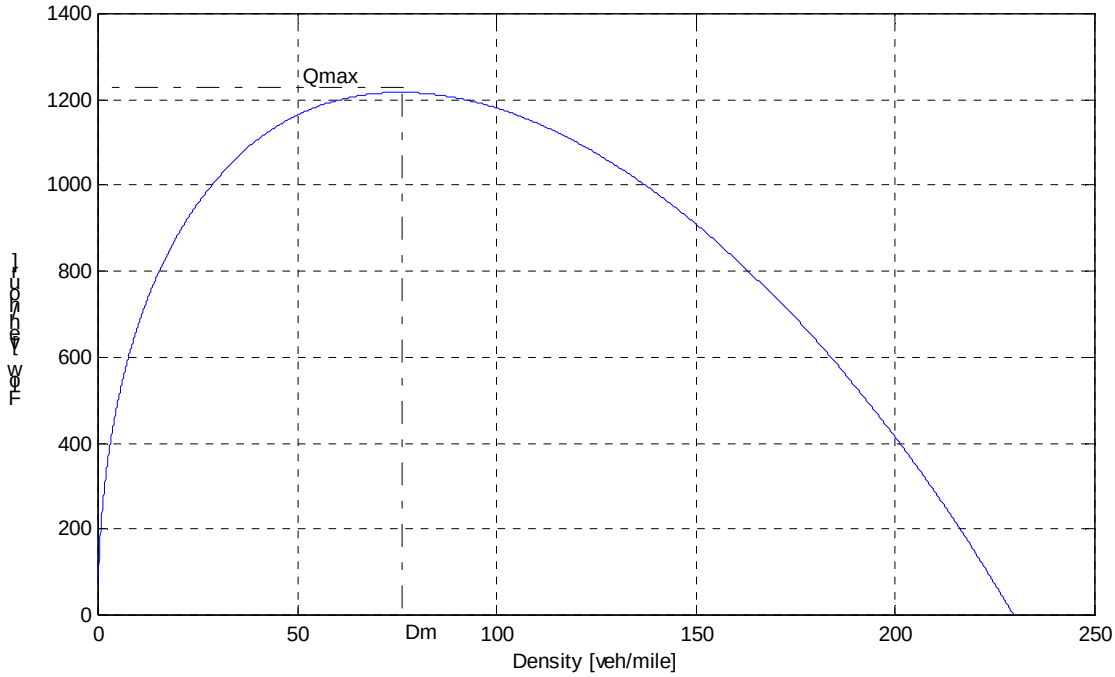

Fig. 4: Flow-Density Curve

Let's investigate the impact of the presence of heavy vehicles on the traffic flow by an example.

Example: Let's assume that the terrain of a freeway is rolling, and the trucks are accounted for 10 percent of the vehicles on the freeway, i.e. $P_T = 0.1$. Let's also assume that trucks are the only heavy vehicles on the freeway, i.e. $P_R = 0$. Using the Highway Capacity Manual (1998), the value of E_T is found to be equal to 3 for rolling terrain freeway. Thus, the heavy traffic adjustment factor would be,

[1] The density or concentration, D, is defined as the ratio of the number of vehicles (here passenger cars) to the length of the roadway segment. It is measured in passenger cars per mile [pc/mi].
[2] Fundamental traffic stream equation is as follows:
$Q=V.D$ where Q is the flow, D is the density and V is the speed of the traffic stream.

$$f_{HV} = \frac{1}{1+0.1(3-1)} = 0.83$$

Figure 5 shows the fundamental flow-density curve with 10% truck penetration, and with 0% heavy vehicles' penetration in a freeway.

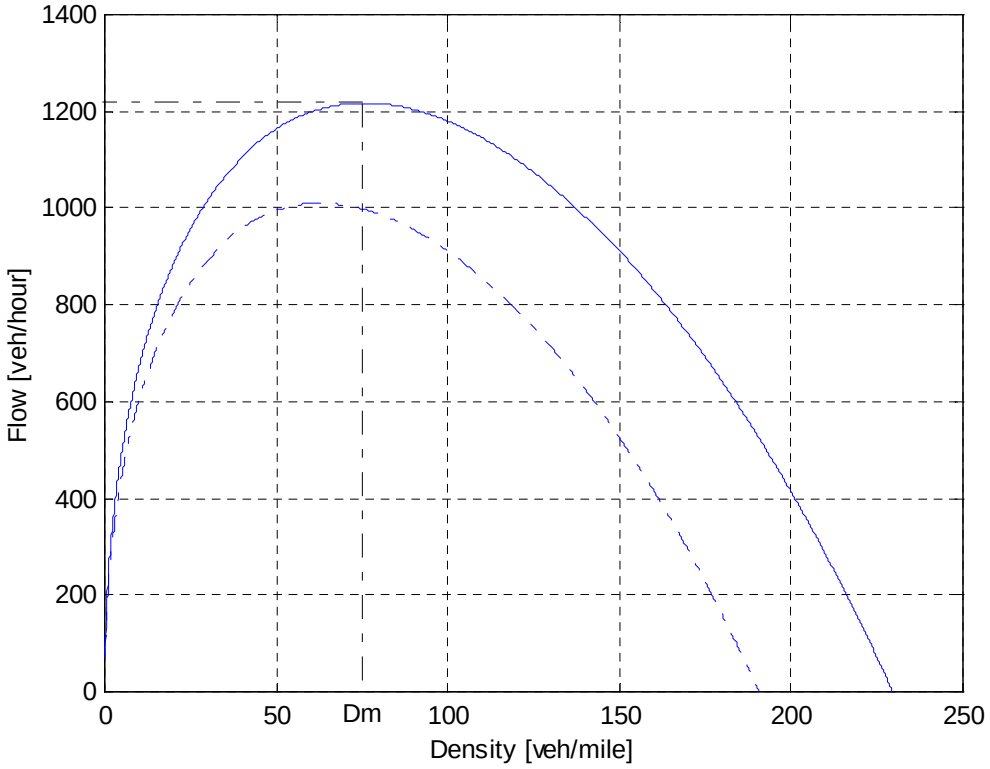

Fig. 5: a) solid line: 0% truck penetration, b) dashed line: 10% truck penetration.

As it is shown in Figure 5, if the density of the highway is close to the origin (free-flow), the effect of the presence of trucks on the traffic flow is negligible. However, as the density of the freeway increases, the presence of the trucks in the freeway has a negative impact on the traffic flow. When the density of the traffic approaches its critical value (density D_m in Figure 5), the flow of the traffic for mixed traffic falls far behind that of the passenger car only traffic. The reduction in the traffic flow rate remains as the density of the mixed traffic increases beyond the critical density. The reduction of the traffic flow rate due to the presence of trucks depends on the value of f_{HV}. This value in turn depends on the percentage of the trucks present, P_T, as well as the freeway conditions characterized by E_T.

3.4 Lane Changing

A "lane change crash" occurs when a merging vehicle attempts to change its lane and strikes or is struck by a vehicle in the adjacent lane. In practice, the possibility of merging collisions can be reduced by adjusting relative velocities and increasing the longitudinal inter-vehicles' spacing. Since roadway capacity is proportional to vehicle speed and inversely proportional to longitudinal inter-vehicle spacing, a large reduction in speed or a large increase in spacing leads to a lower capacity. However, safety cannot be compromised. Thus, the choice of Minimum Safety Spacing (MSS) between vehicles for a collision free environment is important both from safety and capacity point of view.

We study the conditions under which lane changing/merging crashes can be avoided. That is given a particular lane change/merge scenario, we calculate the minimum longitudinal spacing which the vehicles involved in lane changing maneuver should initially have so that no collision, of any type, takes place during the maneuver. We follow the methodology presented in [Jula et al., 2000] to investigate the safe and unsafe regions in lane changing/merging scenario. The analysis in [Jula et al., 2000] assumes that all vehicles involved in lane changing maneuver are passenger vehicles. When different types of vehicles are mixed, the minimum spacing requirements change due to the differences in dynamic characteristics.

Let us consider a lane changing situation where truck *M* in Fig. 6 moves from its current position between vehicles *Lo* and *Fo* to a new position between vehicles *Ld* and *Fd* in the neighboring lane. We refer to vehicles *Ld, Fd, Lo, Fo* and *M* as the leading vehicle in the destination lane, the following vehicle in the destination lane, the leading vehicle in the originating lane, the following vehicle in the originating lane, and the vehicle which must perform the lane-changing (which will be called thereafter the merging vehicle), respectively.

Fig. 6: Pre-lane changing configuration showing position of merging truck *M*.

In order to measure the lateral and longitudinal positions of the vehicles involved in the maneuver an arbitrary origin, denoted by *"O"* in Fig. 6, is selected. The axis *y* (vertical axis) is directed toward the destination lane, and the axis *x* (horizontal axis) is aligned with the lateral side of the merging vehicle that is closer to the destination lane. Fig. 6 shows the top view of the pre-lane changing configuration of the vehicles involved in the lane changing maneuver where the destination lane is assumed to be on the left of the originating lane; the axes *x* and *y* are chosen correspondingly. The origin *"O"* and the axes *x, y* in Fig. 6 are assumed to be fixed during the maneuver.

Hereafter, the longitudinal acceleration/deceleration, the longitudinal velocity, the longitudinal position, and the lateral position of vehicle *i* will be denoted by $a_i(t)$, $v_i(t)$, $x_i(t)$, and $y_i(t)$, respectively, where $i \in \{Ld, Fd, Lo, Fo, M\}$. More precisely, $x_i(t)$ and $y_i(t)$ are, respectively, the longitudinal and lateral distances between the front-left corner of the vehicle *i* and the origin "*O*".

With the exception of the merging truck, the lateral acceleration of all other vehicles is assumed to be zero. The lateral acceleration profile of the merging vehicle is given by (17). We also assumed that all vehicles in both lanes, except vehicle *M*, are moving with constant longitudinal velocity, i.e. $a_i(t)=0$ for $i \in \{Ld, Fd, Lo, Fo, M\}$, while the longitudinal acceleration profile of the merging vehicle, *M*, is the one given by (20). More precisely, the merging vehicle is initially moving with constant longitudinal velocity $a_{adj}=0$. At the time-instant t_{adj} , the merging vehicle starts merging and it accelerates with longitudinal acceleration equal to *acc* . The merging vehicle continues to accelerate at this rate until its longitudinal velocity becomes equal to the velocity of the vehicles in the destination lane at the time-instant $t_{adj} + t_{long}$. After this time the merging vehicle's longitudinal acceleration becomes zero.

$$a_M(t) = \begin{cases} acc & t_{adj} \le t \le t_{long} + t_{adj} \\ 0 & Otherwise \end{cases} \qquad (20)$$

In [Jula et al.,1999] the above profiles for lateral and longitudinal acceleration were considered to find the safe and unsafe regions between the merging vehicle and other vehicles involved in lane changing/merging maneuver where all vehicles were assumed to be passenger cars. In this work, the merging vehicle *M* is a truck as shown in Fig 6 and the results obtained will be compared with those in [Jula et al., 1999] where *M* is a passenger car.

Two scenarios have been considered for the merging maneuver. The first scenario involves collision considerations between the merging vehicle *M* and the leading vehicle *Ld*, and the second involves collision consideration with the following vehicle *Fd* in the destination lane. Both vehicles in the destination lane are considered to be passenger cars, and the merging vehicle is assumed to be either a passenger car or a truck.

Our objective is to find the minimum initial longitudinal spacing, Sr(0), between the merging vehicle *M* and each one of the vehicles in the destination lane such that no collision between *M* and the vehicles in the destination lane will occur.

Fig. 7 shows the safe and unsafe regions between the merging vehicle *M* (car or truck) and the leading vehicle *Ld* (scenario 1). The curves in this figure are the initial minimum safety longitudinal spacing, which divides the relative initial spacing–relative initial longitudinal velocity into safe and unsafe regions. The relative initial longitudinal spacing between *M* and *Ld* is defined as follows:

$Sr(0)=x_{ld}(0)-L_{ld}-x_m(0)$

where L_{ld} is the length of the leading vehicle *Ld*.

As shown in Fig. 7, for positive relative velocity between the merging vehicle and the vehicle in the destination lane, there is almost no difference between the safe and unsafe regions for a passenger car and a truck. For negative values they differ considerably. This is mainly due to the maximum lateral acceleration that a truck can achieve which is much less than that of a passenger car. This fact in turn increases the time needed to perform the lane change maneuver for the merging truck, which results in expansion of the safe region.

By examining the curves in Fig. 7, one can easily see that if the initial relative velocity between *M* and *Ld* is -5m/s (approx. -12 mph), the minimum initial relative spacing for safe lane changing for the merging car and truck will be -11m and -18m, respectively. The associated negative sign of spacing means that the initial longitudinal position of the merging vehicle in the originating lane can be greater (positioned ahead) than that of the leading vehicle in the destination lane, while the lane-changing maneuver can still be safe.

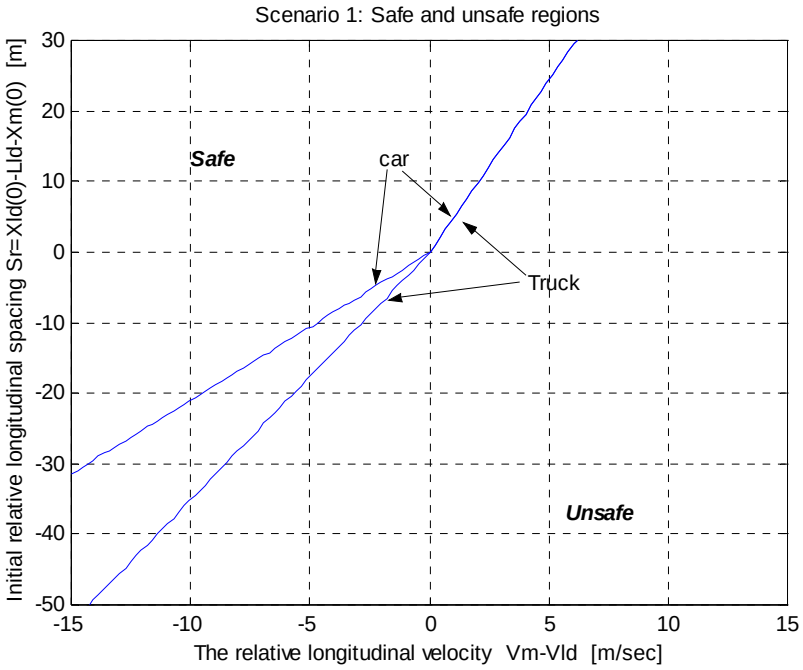

Fig. 7: The safe and unsafe regions between merging vehicle *M* (car or truck) and the leading vehicle in the destination lane.

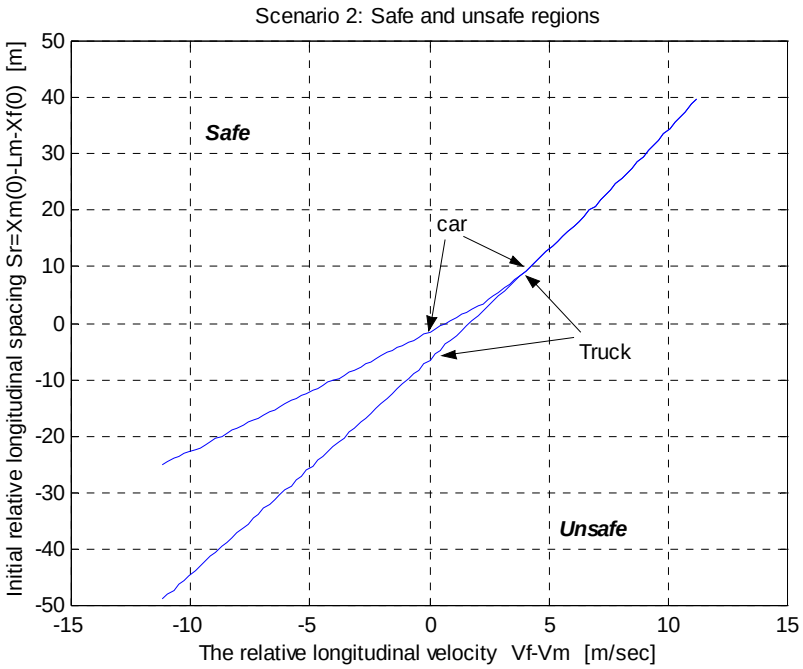

Fig. 8: The safe and unsafe regions between merging vehicle M (car or truck) with following vehicle in the destination line.

In Fig. 8 the safe and unsafe regions between the merging vehicle *M* (car or truck) and the following vehicle *Fd* (scenario 2) are shown. The curves in this figure are the minimum initial safety longitudinal spacing, which divides the relative initial spacing–relative initial longitudinal velocity into safe and unsafe regions. The relative initial longitudinal spacing between *M* and *Fd* is defined as follows:

$$Sr(0)=x_m(0)-L_m-x_{fd}(0)$$

where L_m is the length of the merging vehicle *M*.

Similar to scenario 1 (shown in Fig. 7), in scenario 2 there is also no difference between the safe and unsafe regions for a passenger car and a truck when the relative velocity between the merging vehicle and the following vehicle in the destination lane is positive. Likewise for negative values they differ due to the maximum lateral acceleration that a truck can achieve. Similar considerations as in Fig. 7, explained above, apply to Fig. 8, as well.

4 MICROSCOPIC ANALYSIS OF TRAFFIC FLOW

In this section, we investigate the dynamical interaction between trucks and passenger cars in traffic flow at the microscopic level. Trucks have different dynamical response from passenger cars and have low actuation-to-weight ratio, which translates into lower acceleration. In other words, they have limited acceleration capability and thus may not be able to keep up with accelerating passenger cars. To further investigate and study the effect of the interaction of truck and passenger car dynamics on traffic flow, we simulate different vehicle following scenarios. We use a human driver car following model, namely the Pipes model, to model the responses of passenger vehicles. A brief description of the model is given below followed by simulations. The trucks are modeled using the longitudinal model presented in Section 2.1.

4.1 Pipes Model

This is a linear follow-the-leader model based on car following theory that pertains to single lane dense traffic with no passing and assumes that each driver reacts to a stimulus from the vehicle ahead. The stimulus is the velocity difference and the driver responds with an acceleration command, i.e.

$$Response(t) = Sensitivity \times Stimulus(t - \tau)$$

where τ is the reaction time of the driver-vehicle system.

It can be mathematically expressed as

$$a_f = \frac{\lambda}{M}[v_l(t-\tau) - v_f(t-\tau)] \tag{21}$$

where v_l and v_f are the lead and following vehicle's velocities, respectively, a_f is the following vehicle's acceleration, M is the mass of the following vehicle and λ is a sensitivity factor. The dynamics of the vehicle are modeled by an integrator and the driver's central processing and neuromuscular dynamics by a constant. This model was first proposed by Pipes [Pipes, 1953] and later validated by Chandler [Chandler, 1958]. It has been shown experimentally that the Pipes model closely models passenger car responses during transients [Bose & Ioannou, 2000].

4.2 Driver Model for Trucks

The longitudinal model presented in Section 2.1 models longitudinal truck dynamics. For vehicle following, this model interacts with a driver model that completes the driving loop. However, a driver model specific for trucks is not available in literature. For this reason, we develop a model that incorporates a proportional-Integral (PI) controller assuming that the driver reacts to changes in the lead vehicle speed and inter-vehicle spacing. The model can be expressed as:

$$\dot{v}_{tr}(t) = TD.\left[1 + \frac{0.01}{s}\right]\left(v_{lead}(t - \tau_t) - v_{tr}(t - \tau_t)\right) \quad (22)$$

where v_{tr} is the speed of the truck, v_{lead} is the speed of the lead vehicle, $\dot{v}_{tr}$ is the acceleration of the truck, *TD* is the longitudinal truck dynamics presented in section 2.1 and τ_t is the reaction time (delay) of the truck driver.

Since the truck driver is an experienced personnel sitting higher up than passenger car drivers and able to view 3 to 4 vehicles ahead, the time delay to react to vehicle responses ahead of the truck is lower than the average 1.21 seconds for passenger car drivers [Taoka, 1989]. In our model, we assume a time delay of 1.0 second for the truck driver to respond, i.e. τ_t = 1.0 second. It is important to note that this delay is just the time delay for the driver to react in response to speed and inter-vehicle spacing deviations. The total time for the truck to react is the sum of this delay and the actuator delays.

4.3 Simulations

We simulate a string of 10 vehicles following a lead vehicle in a single lane with no passing. Furthermore, we assume dense traffic conditions in which the driver of each vehicle tries to match the speed of the vehicle ahead. The dynamics of the passenger cars are modeled using the Pipes model. The response of the trucks during vehicle following is modeled using the driver model presented above. Initially the vehicles are traveling at 15m/s (~34 mph). Then the lead vehicle accelerates at 0.1g to 25m/s (~56 mph). We study the upstream propagation of the transients generated by the lead vehicle.

First we consider homogeneous traffic with 100% passenger vehicles. As seen in Fig. 9, the passenger cars closely follow the target speed trajectory. Next we assume that the 4th vehicle is a truck (weighing 40 tons) that corresponds to a penetration of 10% in mixed passenger car/truck traffic. The lead vehicle performs the same maneuver and the rest follow suit. As seen in Fig. 10, the truck with its limited acceleration cannot keep up with the passenger car in front of it and falls behind. This creates a large inter-vehicle spacing between the truck and the passenger car ahead (shown in Fig. 11) that may invite cut-ins from neighboring lanes. This is expected to cause further disturbances in traffic flow. Furthermore, the sluggish response of the truck retards the response of the following vehicles. Once the lead vehicle reaches a steady state cruising speed, the truck tries to catch up with it and reduces the inter-vehicle spacing by increasing its speed above the target speed (Fig. 10).

Next we consider that both the 4th and the 7th vehicles are trucks that correspond to a penetration of 20% in mixed passenger car/truck traffic. The lead vehicle performs the identical maneuver as above and the rest follow suit. As shown in Fig. 11, the presence of another truck does not significantly affect the dynamical response of the last vehicle (v10

in Fig. 12) in comparison to the case when there is only a single truck (Fig. 10). Furthermore, the inter-vehicle spacing of the second truck in the 7th position is much smaller than that of the first truck in the 4th position (Fig. 13). In other words, the first truck absorbs the fast acceleration transients generated by the lead vehicle and converts it into a smoother one that can be easily tracked by another truck.

Trucks undergo various degrees of loading; hence their total weight can change depending on the cargo they carry. To determine the effect of weight on the dynamical response of a truck, we consider a single truck carrying a lighter cargo in the 4th position (10% penetration) and weighing 30 tons instead of the previously used value of 40 tons. As shown in Fig. 14, the lighter truck has a faster response than a heavier truck (Fig. 10).

The total distance traveled in a fixed time horizon is shown for the different cases considered above. In Fig. 15 it is observed that the presence of a truck increases the total travel time of the 10th vehicle in comparison to the 100% passenger car traffic. Fig. 16 shows that the total travel time of the 10th passenger vehicle is greater when it is following a heavier truck than a lighter one.

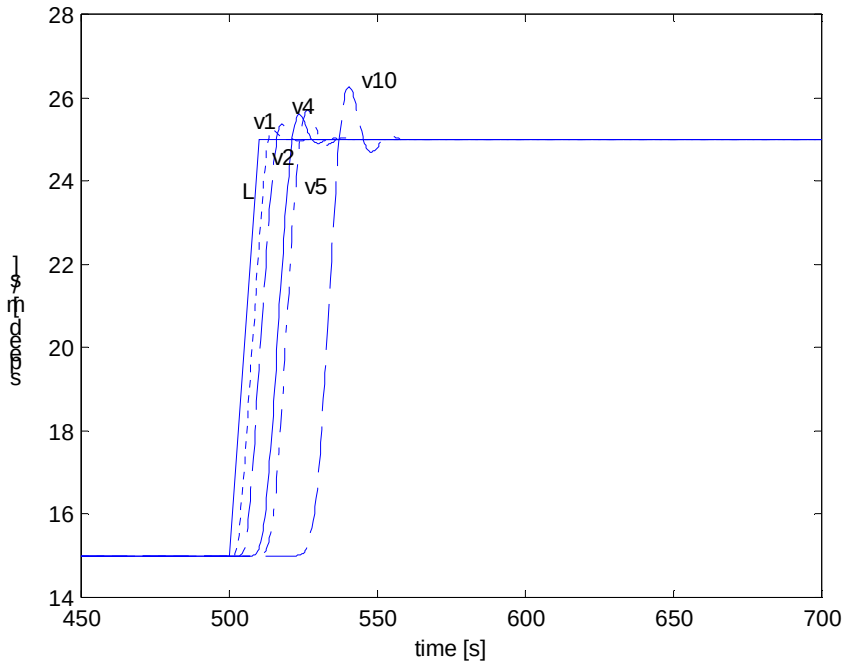

Fig. 9: Vehicles in homogeneous traffic (Pipes model) following a lead vehicle. Velocity response of leader (L), 1st vehicle (v1), 2nd vehicle (v2), 4th and 5th vehicles (v4 & v5) and the 10th vehicle (v10).

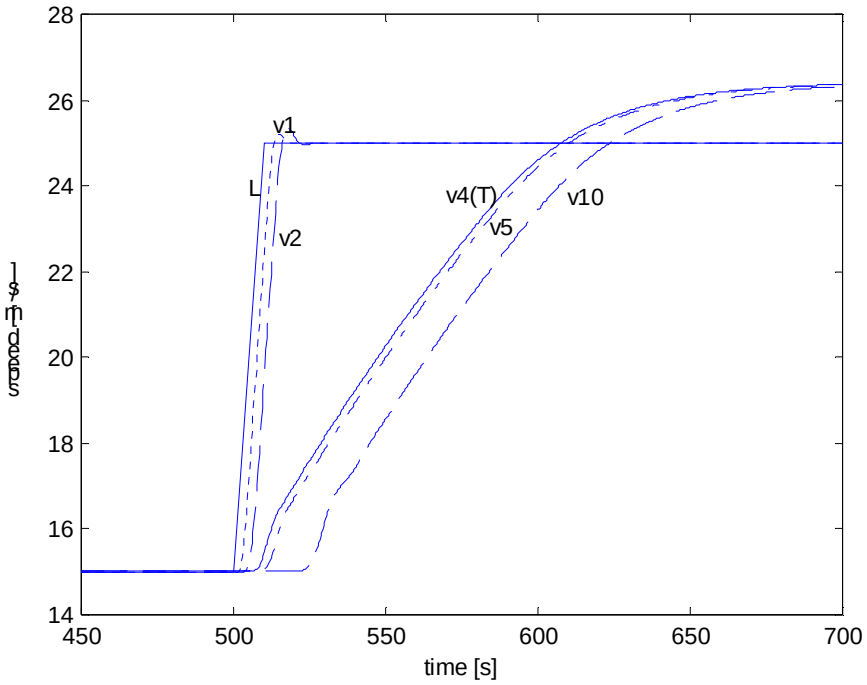

Fig. 10: Vehicles in heterogeneous truck/passenger car traffic (Pipes model) following a lead vehicle.The 4th vehicle is a truck weighing 40 tons. Velocity response of leader (L), 1st vehicle (v1), 2nd vehicle (v2), 4th and 5th vehicles (v4 & v5) and the 10th vehicle (v10).

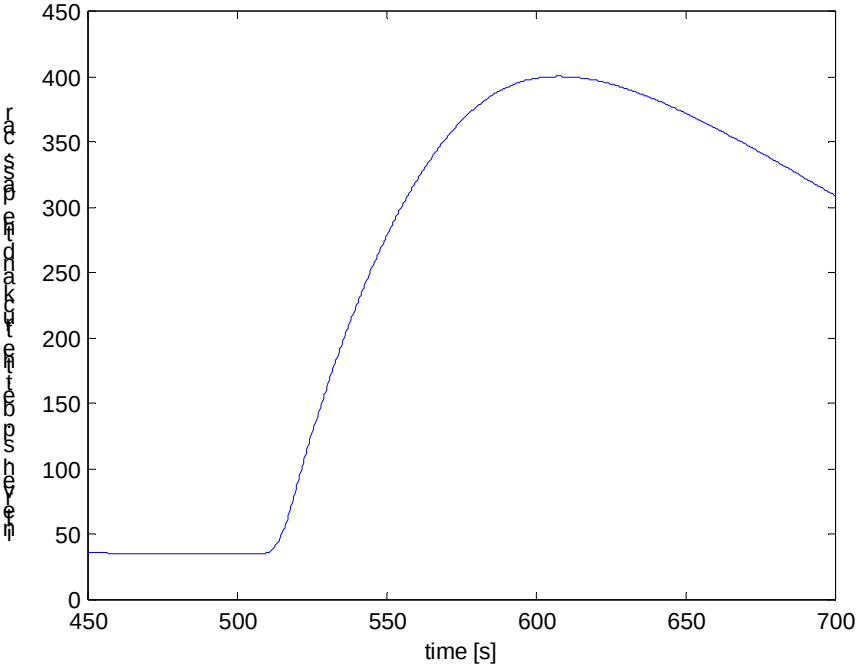

Fig. 11: Vehicles in heterogeneous truck/passenger car traffic (Pipes model) following a lead vehicle.Intervehicle spacing between the truck (weighing 40 tons) in the 4th position and the passenger car in the 3rd position.

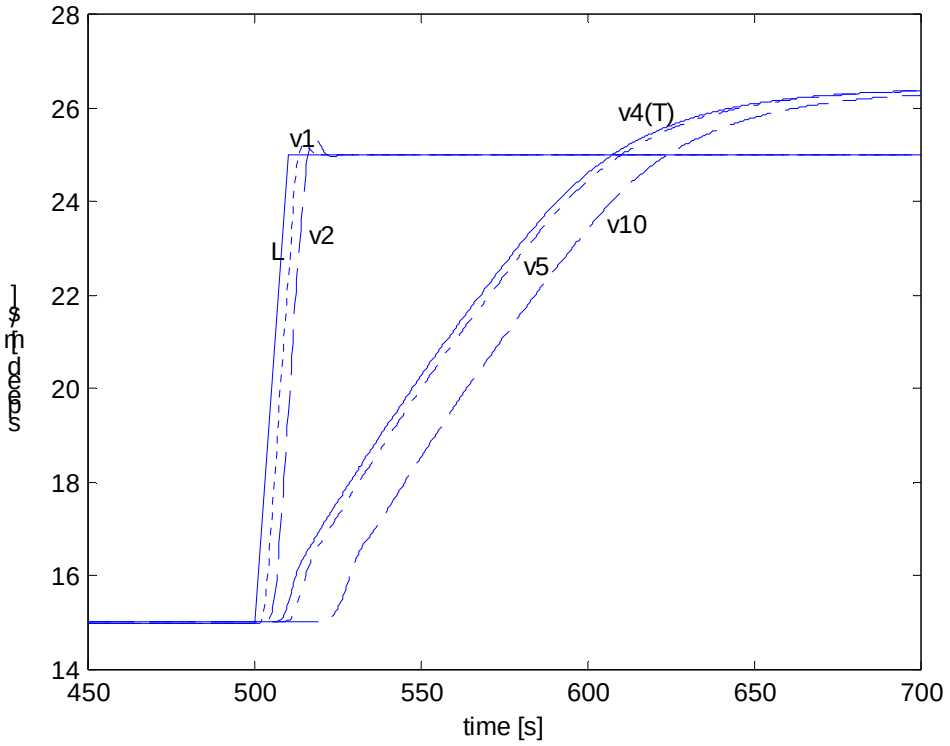

Fig. 12: Vehicles in heterogeneous truck/passenger car traffic (Pipes model) following a lead vehicle.The 4th & 7th vehicles are trucks weighing 40 tons. Velocity response of leader (L), 1st vehicle (v1), 2nd vehicle (v2), 4th and 5th vehicles (v4 & v5) and the 10th vehicle (v10).

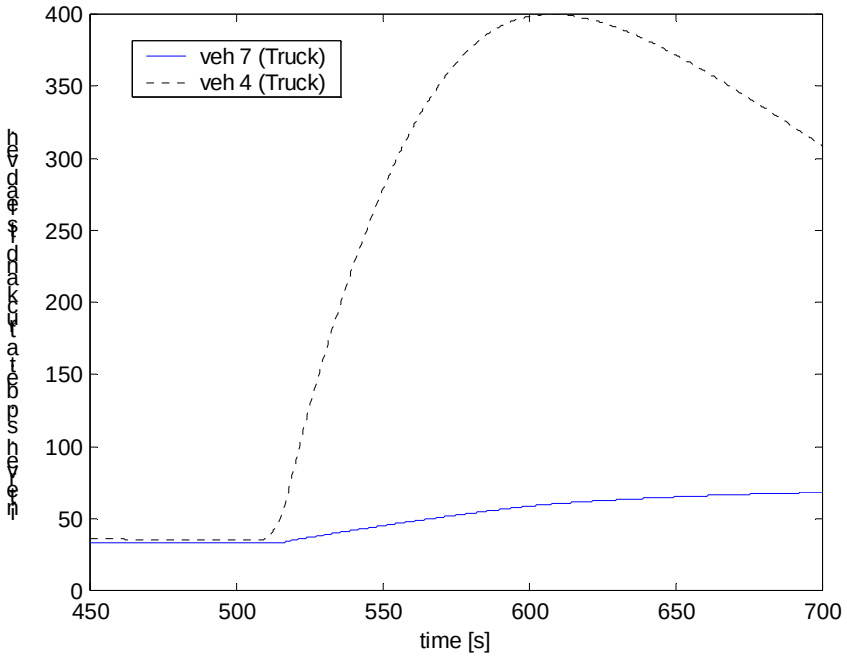

Fig. 13: Vehicles in heterogeneous truck/passenger car traffic (Pipes model) following a lead vehicle.Intervehicle spacing between the trucks (weighing 40 tons) in the 4th & 7th positions and their respective lead passenger cars.

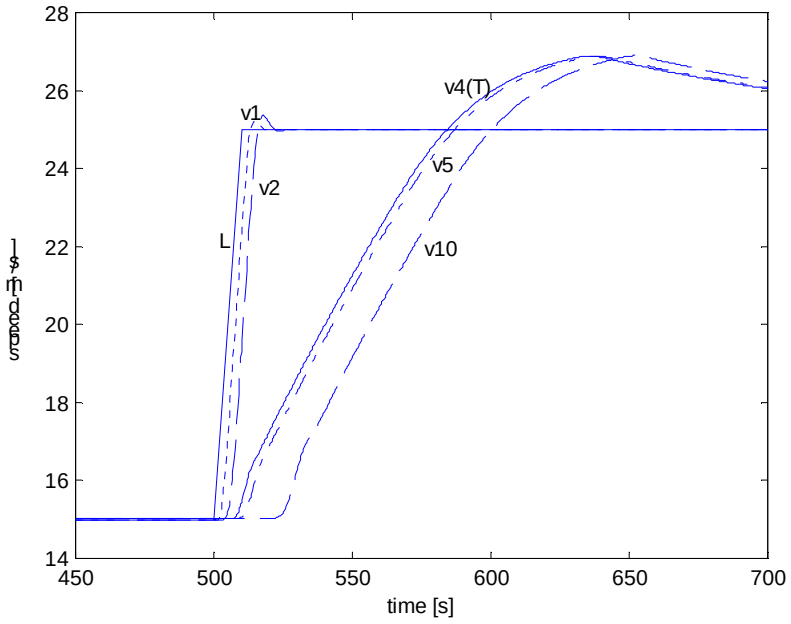

Fig. 14: Vehicles in heterogeneous truck/passenger car traffic (Pipes model) following a lead vehicle.The 4th vehicle is a truck weighing 30 tons. Velocity response of leader (L), 1st vehicle (v1), 2nd vehicle (v2), 4th and 5th vehicles (v4 & v5) and the 10th vehicle (v10).

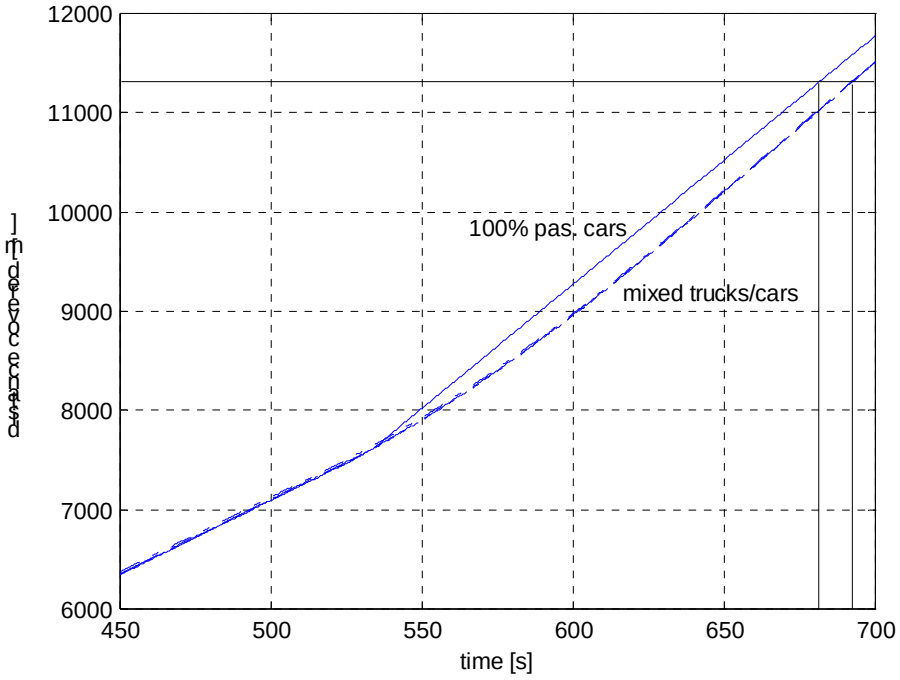

Fig. 15: Vehicles following each a lead vehicle in a single lane.The distance covered by the 10th vehicle in homogeneous and heterogeneous truck(weighing 40 tons)/passenger car traffic.

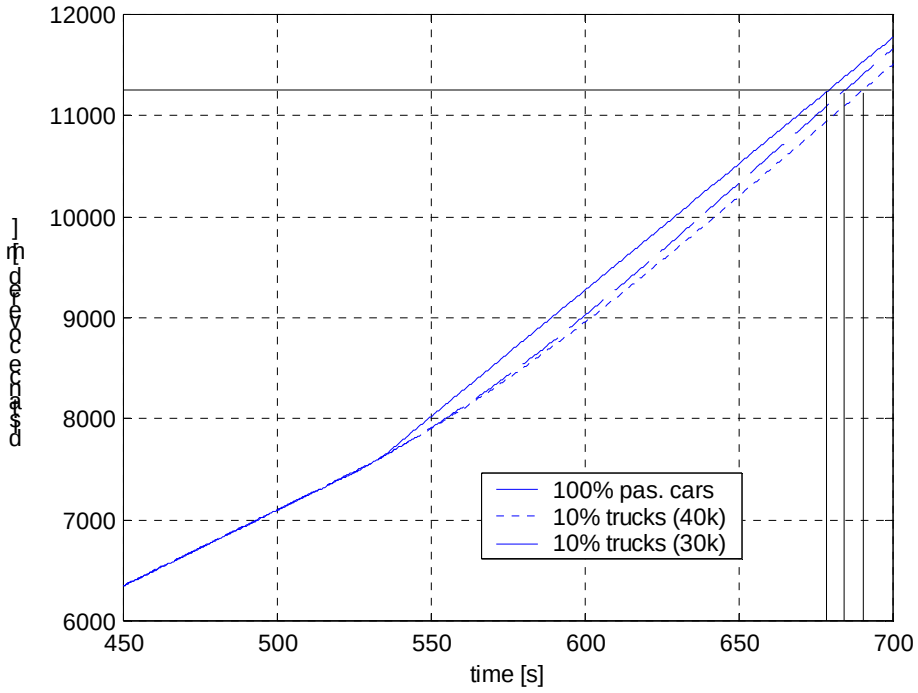

Fig. 16: Vehicles following each a lead vehicle in a single lane.The distance covered by the 10th vehicle in homogeneous and heterogeneous truck/passenger car traffic. The truck weighs 30 tons in one case and 40 tons in the other.

5 MACROSCOPIC ANALYSIS OF TRAFFIC FLOW

In this section, we investigate the effect of mixing trucks with passenger cars at the macroscopic level. In particular, we look at the effect of the presence of trucks that have low actuation-to-weight ratio on the propagation of disturbances in traffic flow introduced by factors such as highway configurations (for example, merging traffic, number of lanes reduced). Such disturbances can affect the travel time, driver stress level and even fuel consumption and air pollution. Minor disturbances caused by speed changes in vehicles are easily absorbed by the nearby vehicles through the active action of the drivers. Major disturbances introduced by sudden changes in the traffic flow, however, generate transient conditions that can develop into shock waves [Lighthill & Whitham, 1955].

In our analysis, we compare two types of traffic. The first is homogeneous traffic consisting of passenger vehicles with similar dynamic characteristics. The second is mixed truck/passenger car traffic that consists of trucks sharing the same lanes with passenger cars.

5.1 Shock Waves

Shock waves are discontinuous waves that occur when traffic on a section of a road is denser in front and less dense behind. The waves on the less dense section travel faster than those in the dense section ahead and catch up with them. Then the continuous waves coalesce into a discontinuous wave or a 'shock wave' [Lighthill & Whitham, 1955]. It can be shown that shock waves travel at a speed given by

$$u = \frac{\Delta q}{\Delta k} \tag{23}$$

where Δq and Δk are the traffic flow and traffic density differences, respectively,

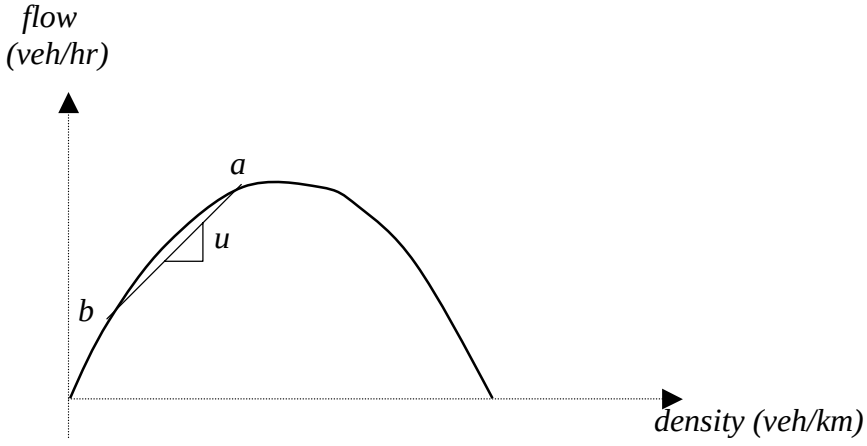

Fig. 17 : Shock wave in homogeneous traffic.

between the two sections. In the fundamental diagram for homogeneous traffic with 100% passenger cars, this is given by the slope of the chord joining the two points that represent conditions ahead and behind the shock wave at *a* and *b*, respectively (Fig. 17).

The question that we pose is: how does the mixing of trucks and passenger cars affect the generation and propagation of shock waves. We answer the question using space-time diagrams that represent vehicle trajectories. This simple theory of traffic evolution will provide an insight into the effect of trucks among passenger cars on the propagation of shock waves. The theory is also used in [Cassidy, 1999] and is a version of one originally developed in [Lighthill & Whitham, 1955]. It is presented in a graphical way and assumes the following: no overtaking and vehicles of the same class exhibit identical headways, spacings and velocities within a given state.

Fig. 18(a) shows the space-time graph for 5 vehicles in homogeneous traffic with 100% passenger cars. At time instant t_d there is a disturbance that causes the lead vehicle to slow down, denoted by a change in slope in the diagram. We assume that the vehicle decelerations occur instantaneously. After a time lag τ_{car}, the following vehicle reacts and decelerates to maintain the inter-vehicle spacing depending on a constant headway policy. Likewise, the rest of the vehicles respond as shown. The shock wave that exists at the boundary of the two regions moves back at a speed given by the slope of the arrow in Fig. 18(a).

For mixed trucks/passenger cars traffic shown in Fig. 18(b), the lines marked '*tr*' denote trucks while the rest are passenger cars. As before, the disturbance at t_d causes the first vehicle to slow down. The following truck reacts after a time τ_{tr}, where $\tau_{tr} > \tau_{car}$, i.e. larger than the time lag for passenger cars. This is so because of the large actuation delay in heavy-duty trucks in comparison to light-duty passenger cars. This effect continues upstream with the trucks taking a larger time to react to speed changes. As shown in Fig. 18(b), the resultant effect is that the average slope of the shock wave decreases and as a result it travels upstream at a lower speed than in Fig. 18(a).

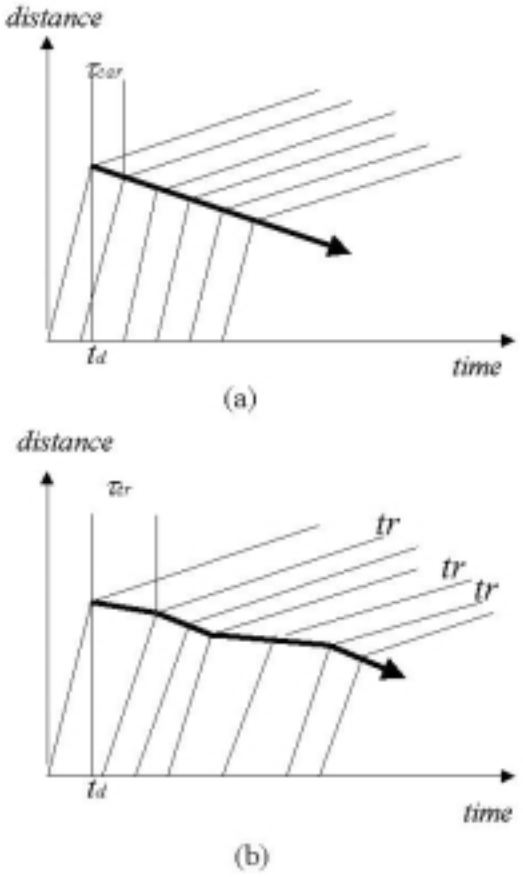

Fig. 18: Space-time graph showing traffic evolution and the propagation of shock waves in (a) homogeneous traffic and (b) mixed traffic.

This phenomenon is illustrated in a three-dimensional representation of the space-time diagram. We construct an axis of cumulative number of vehicles at three different distance points and at three different time instances. The surface of the cumulative vehicle count $N(x,t)$ is staircase-shaped, with each step representing a vehicle trajectory. It follows that if the surfaces are taken to be continuous, then the traffic flow at a given point can be obtained from the $N(x,t)-t$ diagrams directly by using

$$q_x(t) = \frac{\partial N(x,t)}{\partial t} \tag{24}$$

and the traffic density at a given time can be obtained from the $N(x,t)-x$ diagrams using

$$k_t(x) = -\frac{\partial N(x,t)}{\partial x} \tag{25}$$

We use a negative sign in (25) because the cumulative vehicle count is considered by counting the number of vehicles that have not yet crossed the line at a time instance *t* in the space-time diagrams. This is the number of vehicles to the left of *t,* which is opposite to the motion of the vehicles and hence the negative derivative.

It is important to note that the continuum approximation to a discrete flow is valid only in the regime of dense traffic. Writing (24) and (25) together, we obtain the continuity equation

$$\frac{\partial q}{\partial x} + \frac{\partial k}{\partial t} = 0 \tag{26}$$

The cumulative vehicle count curve $N(x_2,t)$ for the point x_2 in the $N(x,t)-t$ diagrams in Fig. 19 is obtained by shifting the curve $N(x_1,t)$ horizontally to the right by the time it takes a vehicle to travel from x_1 to x_2. However, this is not the proper representation of the cumulative curve at x_2 due to the presence of the shock wave. Thus we perform the following transformations. We shift the cumulative curve $N(x_3,t)$ for x_3 (a point after the shock wave) horizontally to the right by the time it takes the shock wave to travel from x_3 to x_2, and vertically upwards by the number of vehicles that cross the shock wave interface. The number of vehicles that cross the shock wave interface is given by the product of traffic density in the region after the shock wave and the distance from x_2 to x_3. This curve is then combined with $N(x_2,t)$ to obtain the correct cumulative curve $N'(x_2,t)$ at x_2. We use a similar procedure to construct the cumulative vehicle count curve $N(x,t_2)$ at time instant t_2 in $N(x,t)-x$ diagrams in Fig. 19. The cumulative *N*-curves are the ones that will be observed if vehicles counts are taken using measurement devices at positions x_1, x_2 and x_3 at time instances t_1, t_2 and t_3.

We observe from the cumulative curves in Fig. 19 that the traffic flow and traffic density is lower in mixed truck/passenger car traffic than in homogeneous passenger car traffic. Furthermore, we observe from the $N(x,t)-t$ diagrams that the traffic flow at a given point decreases less rapidly in mixed traffic than in homogeneous traffic. Likewise, from the $N(x,t)-x$ diagrams, we can conclude that the rate of increase in traffic density is lower in mixed traffic than in homogeneous traffic. These are consequences of the shock wave traveling slower in mixed traffic than in homogeneous traffic.

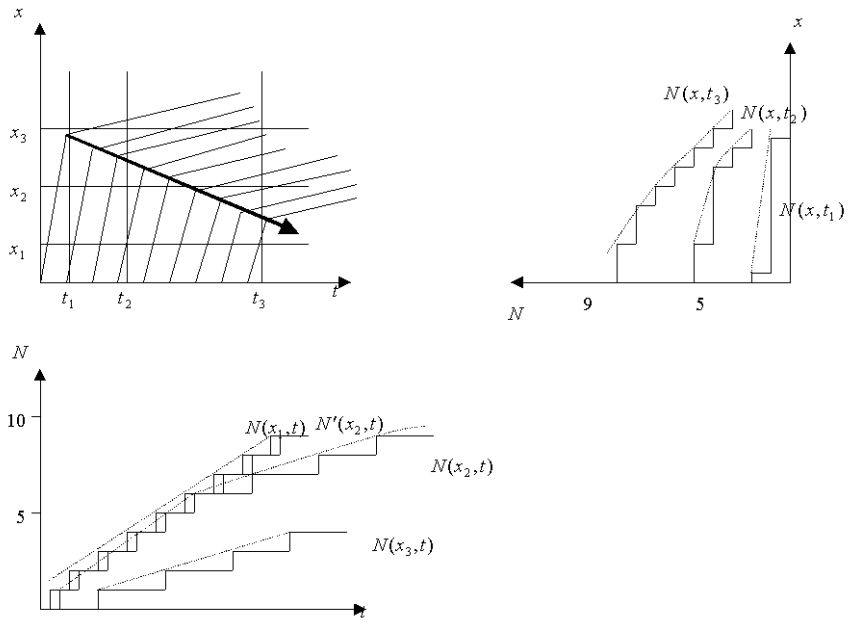

Fig. 19(a): Three-dimensional representation of homogeneous traffic.

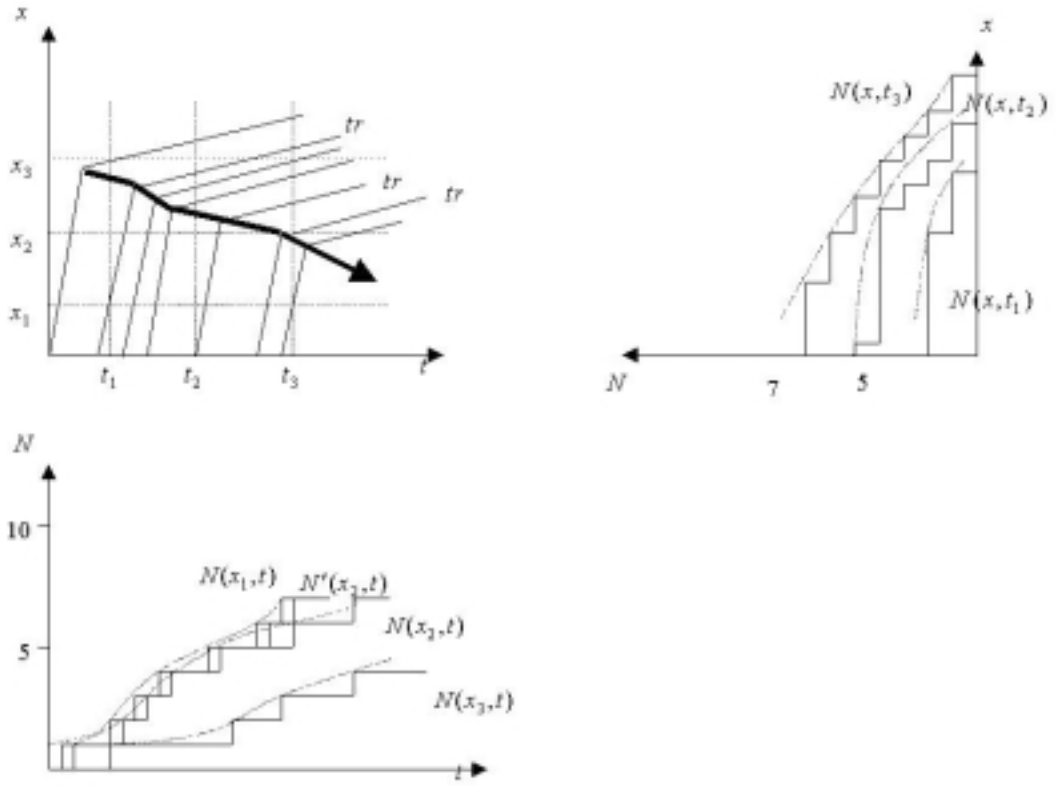

Fig. 19(b): Three-dimensional representation of mixed traffic.

5.2 Simulations

Traffic flow simulations are performed to demonstrate the theory propounded in the previous section. Consider a stretch of road of length 2.5 km subdivided into 5 sections of 500m each. A constant traffic flow is assumed along the road. The manual vehicle dynamics are modeled using the Pipes linear car-following model from [Pipes, 1953; Chandler, 1958]. It has been shown experimentally that the Pipes model models human driver responses during transients [Bose & Ioannou, 2000]. A simplified and linearized model of the nonlinear truck model used in Section 4.3 is used in the macro simulations.

The reaction time for passenger cars is taken to be equal to the reaction time of a driver which is 1.21 seconds [Taoka, 1989]. On the other hand, the reaction time for trucks is taken from section 3 and is equal to 1.7 seconds. All vehicles follow a constant headway policy. The headways for the passenger car are generated according to a lognormal distribution given in [Cohen, 1991]. Typically large semi-trailer trucks have varied length from 55 ft to 74 ft [ITE Technical Council Committee, 1992]. While following a vehicle on the highway, the "usual practice" for trucks is to use inter-vehicle spacing (i.e. the distance from the lead vehicle) two to three times the truck length. However, this again varies from driver to driver and is dependent on weather, road conditions, among others. While such considerations give a broad range of headway for trucks, for our study we take a headway that is within the acceptable range for truck driver and is equal to 2.6 seconds. It is important to note that the headway defined in [Cohen, 1991] is the time taken to cover the distance that includes the vehicle length. The maximum value for the passenger car headway is taken as 2.5s. This is done to make the study applicable to current passenger car traffic where seldom a vehicle in moderately dense traffic conditions uses a headway greater than 2.5s. On the other hand, truck drivers are experienced personnel with less variability in driving characteristics and thus all trucks are assumed to use the same time headway of 2.6 seconds.

In our simulations we calculate the traffic flow rate and the average traffic speed in each section. To calculate the traffic flow rate, we count the number of vehicles crossing a point of the highway. Assuming a detector at the end of section 5 on the road, we count the number of vehicles that cross the end of section 5 over a specified time interval and then average that to get the flow rate in veh/hr/lane. The specified measurement interval for traffic flow is taken to be 60 seconds. The simulation is run for 600 seconds, which gives 10 measurements of traffic flow. We first consider 100% passenger car and then mixed truck/passenger car traffic with 10% trucks that are placed randomly among the passenger cars.

Initially all vehicles are traveling at 15m/s. Then after 60 seconds when the first traffic flow count has been measured, the lead vehicle in section 5 accelerates away rapidly at 0.1g and the rest of the vehicles follow suit. In mixed traffic, if the lead vehicle in section 5 is a truck, then it accelerates at its maximum value of 0.01g. The following vehicles try to follow the vehicle ahead while at all times maintaining an inter-vehicle spacing stipulated by the time headway policy.

In Fig. 20 and Fig. 21 we plot the time headways of the vehicles on the highway at the start of the simulation in homogeneous and mixed truck/passenger car traffic, respectively. As seen, there are numerous manual vehicles with time headway 2.5 seconds, since that is the stipulated upper limit. Also in Fig. 21 the trucks can be seen with time headway of 2.6 seconds.

Fig. 22 shows the traffic flow in 100% passenger car and mixed traffic/passenger car. As expected, the average traffic flow is higher in 100% passenger car traffic than in mixed truck/passenger car traffic. This happens since the trucks are longer than passenger cars and also since they use larger time headway and thus a larger inter-vehicle spacing than passenger cars. Fig. 23 shows the average traffic speed in 100% passenger car and mixed truck/passenger car traffic. The average traffic speed in Section 5 gradually increases following the disturbance. However, the rate of increase is higher in 100% passenger car traffic than in mixed truck/passenger car traffic. This is due to the slower truck dynamics and its limited acceleration. Fig. 24 is a cross section of the 3-D plot of the average speed profile in section 5. It has numerous spikes followed by deep valleys because of the following. The gradual increases in the speed profile leading to the peaks occur when the lead vehicle in section 5 is a passenger car that accelerates at 0.1g and generates a high-speed gradient. The deep valleys account for the case when the lead vehicle in section 5 is a truck that accelerates at 0.01g and retards the speed increase in the section. It can be observed that the average speed in section 5 is higher in 100% passenger car traffic than in mixed truck passenger car traffic due to the limited truck acceleration.

The shock wave that develops in section 5 can be observed traveling upstream at a faster rate in 100% passenger car traffic than in mixed truck/passenger car traffic. As a result, the average increase in average traffic speed spills over in section 4 in 100% passenger car traffic. This demonstrates the theory explained using Fig. 18.

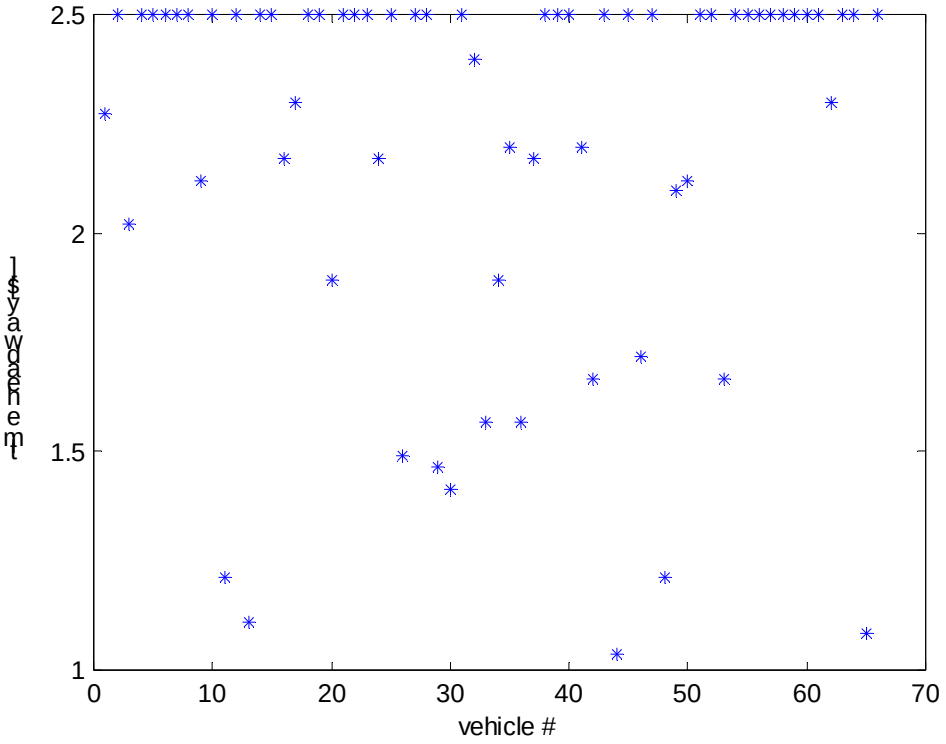

Fig. 20 : Time headway of vehicles in homogeneous passenger car traffic.

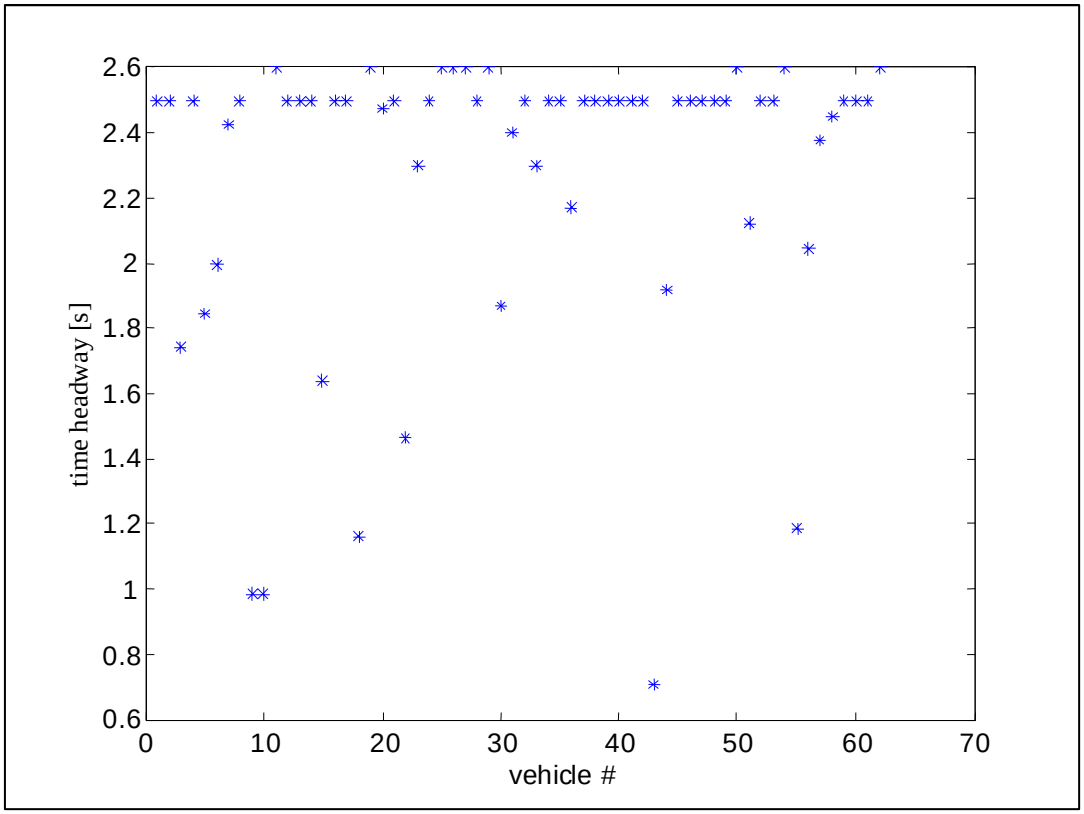

Fig. 21 : Time headway of vehicles in heterogeneous truck/passenger car traffic.

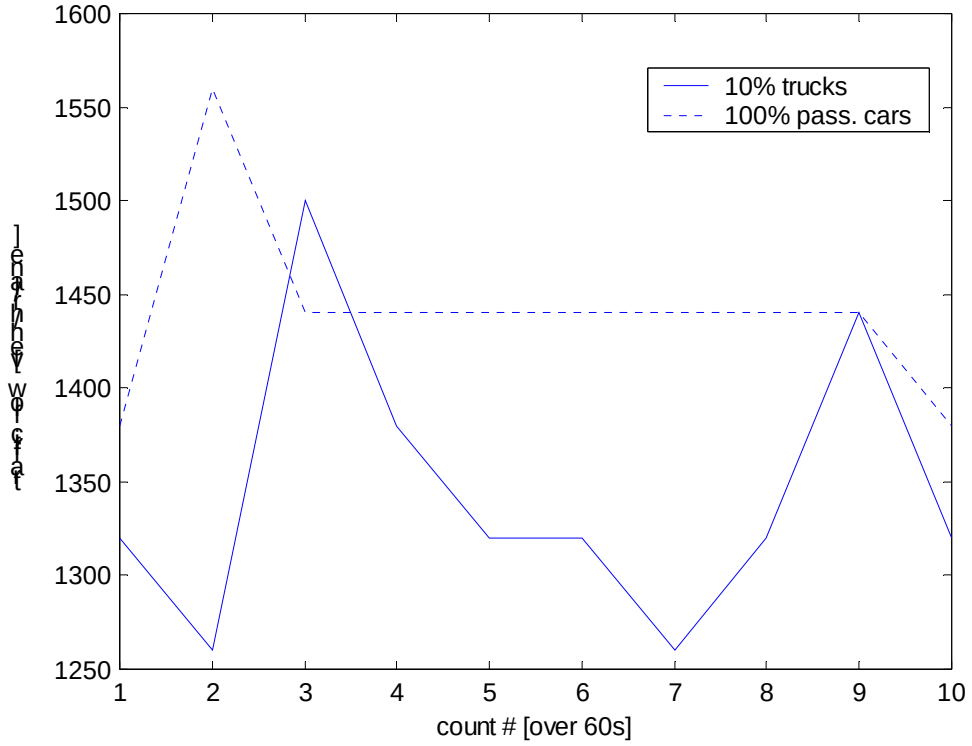

Fig. 22 : Homogeneous and heterogeneous truck/passenger car traffic flow.

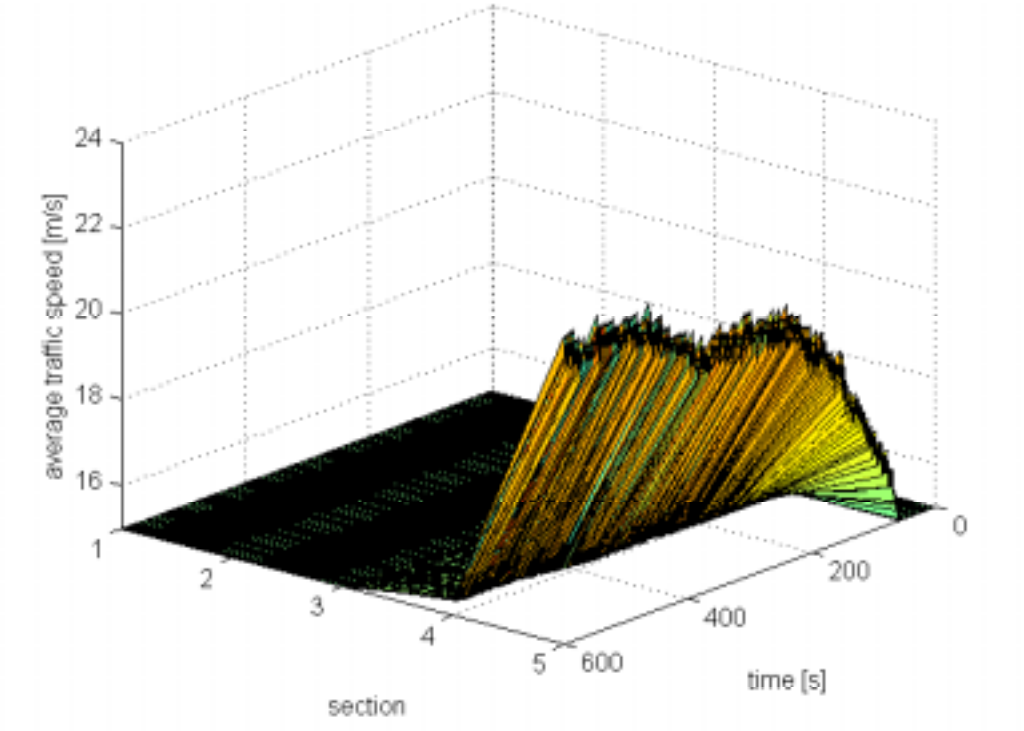

(a)

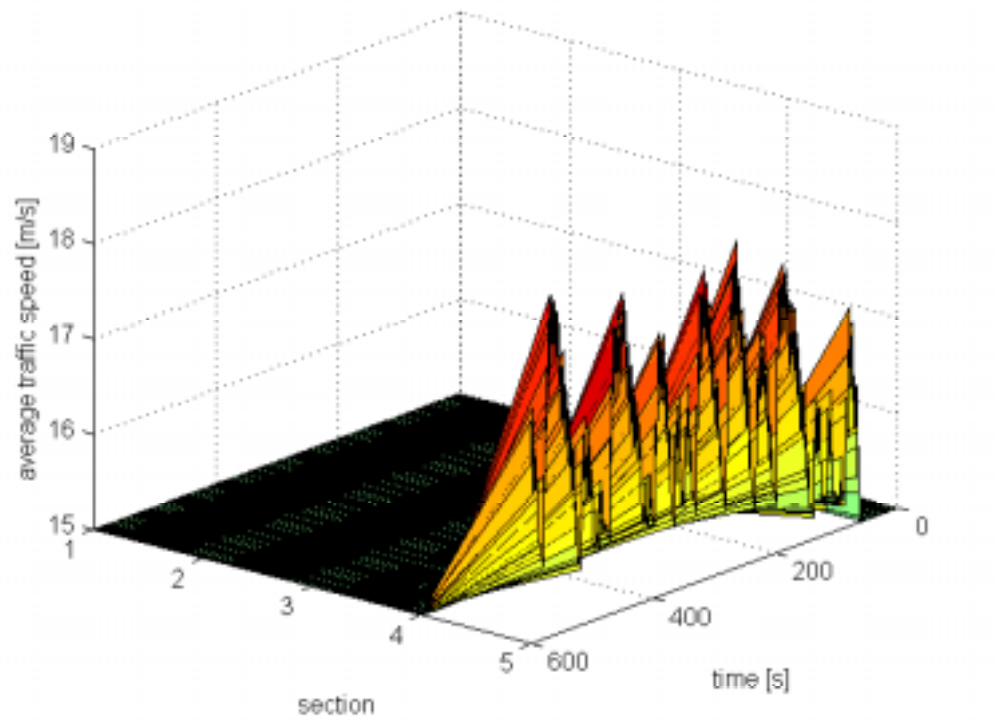

(b)

Fig. 23 : Average traffic speed in 5 sections in (a) homogeneous and (b) heterogeneous truck/passenger car traffic when the lead vehicle in section 5 accelerates.

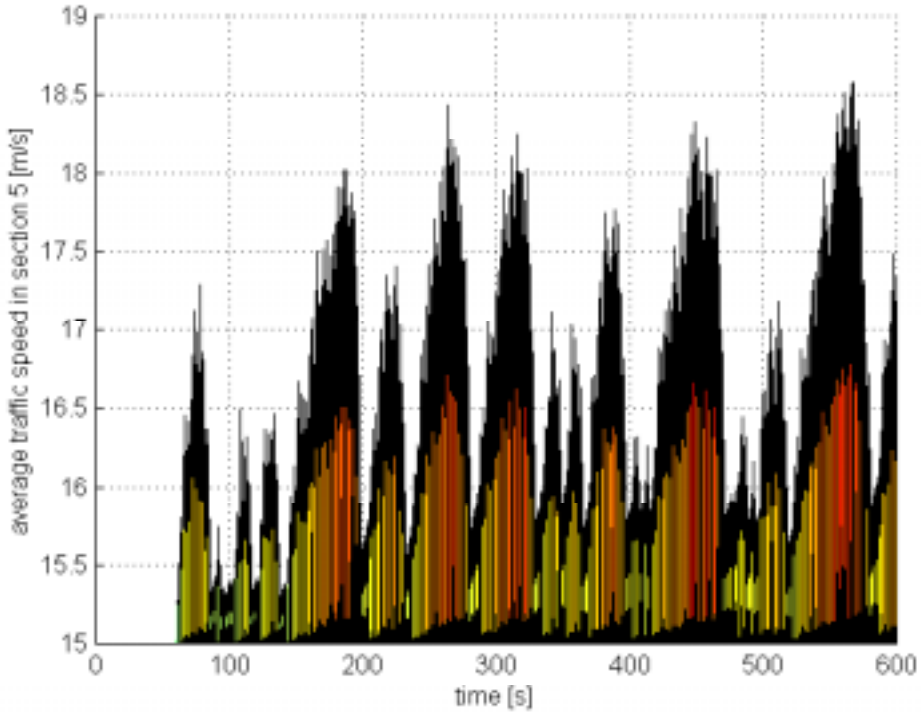

Fig. 24 : Average traffic speed in section 5 of the highway in heterogeneous truck/passenger car traffic when the lead vehicle in section 5 accelerates.

6 Conclusions and Recommendations

We have shown analytically and demonstrated via simulations both on the microscopic and macroscopic level that trucks have a negative effect on highway traffic flow rate for traffic streams involving passenger cars and trucks. Their “sluggish” dynamical response, size and high inertia affect safety and cause traffic disturbances during transients that could lead to shock waves and lower traffic flow rates.

Our results on the effect of trucks on traffic flow rates and capacity are in good agreement with empirical data presented in the Highway Capacity Manual.

The results developed are based on assumed truck and driver models, which are validated with actual data. Since there is a variety of trucks, the assumed truck model does not model all possible trucks. Consequently our results could be viewed as qualitative rather than quantitative.

The dynamical characteristics of trucks during turns, and acceleration/deceleration maneuvers are taken into account in part II for developing dynamic routing algorithms for trucks.

PART II: DYNAMIC ROUTE GUIDANCE

1 INTRODUCTION

Traffic congestion is one of the main problems encountered by the trucking industry, and it affects the industry along three major dimensions: (a) transit time; (b) reliability; and (c) cost. Trucking is a commercial activity, and trucking operations are driven by the need to satisfy customer demands for pickup and delivery times, and by the need to operate at the lowest possible cost [Meyer et al., 1996]. The trucking industry is highly competitive, with easy entry into almost any market, relatively little differentiation between operators and slim profit margins. A trucker who cannot meet customer demands or cannot operate at a competitive cost will go out of business. Truck operating patterns and the daily choices made by truck drivers are, to a great extent, made on the basis of satisfying the customer needs at a low cost.

When selecting routes, truck drivers often attempt to outsmart the other drivers in order to avoid congestion, but in most cases, drivers lack the information needed to make the right decisions concerning route selection. Dispatchers play a major role in informing drivers about traffic conditions, in addition to assisting them in departure/arrival decisions and providing navigational information [Ng. et al., 1995]. Dispatchers currently obtain information about traffic conditions, mostly through radio traffic reports and through information relayed back by the drivers [Hall and Intihar, 1997]. As the information technology infrastructure becomes more sophisticated, however, more accurate real-time information about traffic incidents and traffic congestion will be available at all times. The dispatcher, aided by appropriate software and routing algorithms, will have an accurate picture of where non-recurring and recurring congestion exists at any time, and will be able to direct the driver around the congestion points. Rerouting drivers to avoid congestion improves the productivity of the firm as well as of the individual driver, with resulting improvements in customer service, reduction in costs, reduced fuel consumption and the corresponding benefits to the environment. [Batz, 1991].

A *Route Guidance System* (RGS) is a technical system that supports the three main activities of a truck driver who travels from an origin to a destination point:

(1) *Route Planning*. This is the initial selection of the route, before the beginning of the trip. This planning is usually based on a map of the area, or based on familiarity of the driver with the area. The route selection is made according to certain pre-specified criteria on part of the driver, such as minimum distance or faster arrival.
(2) *Navigation*. During the trip the driver finds and follows the selected route.
(3) *Re-Planning or Route Guidance*. During the trip, the initially selected route may need to change due to unforeseen problems on the road, such as traffic congestion or other considerations.

Depending on the way the available information is being used and route decisions are made, route guidance systems can be classified as:

- *Distributed RGS*: any available information is sent directly to the vehicle, where an on-board computer calculates the "optimal" route according to certain pre-specified criteria. This is a "user oriented" guidance system.
- *Centralized RGS*: the information is being processed at a traffic information center, where the "optimal" routes for all vehicles controlled by the center are calculated and the route decisions are conveyed back to the drivers. This is a "system oriented" RGS.

In this project we develop a RGS for objectives (1) and (3) above, i.e. for initial route planning and route re-planning, and we apply it, as a case study, to a real traffic network in a commercial area of the Los Angeles region. The area under study is highly traveled and includes surface streets and freeway segments. The developed system can be used as a distributed RGS tool, since it deals with the routing of a single vehicle. Objective (3), the route re-planning activity, is termed "dynamic route guidance", since it uses information dynamically, as soon as it becomes available, and it is continuously recalculating the optimal route. Objective (1), the initial route planning activity, is termed "static planning", since it calculates the route once, based on the information available at the beginning of the trip, without updating the route during the trip. The optimality criterion used for both objectives is "minimum travel time", rather than minimum geometric distance.

In this study a deterministic approach to traffic routing has been used. Assuming we have valid deterministic data about typical traffic conditions throughout the network, we will use these data for initial route planning. The deterministic time-dependent shortest path problem has been addressed by Dreyfus (1969), Cook & Halsey (1969), Lawler(1976), and Kaufman & Smith (1993), among others. In section 3 we address a similar deterministic time-dependent shortest path problem and demonstrated the approach for a traffic network in the Los Angeles area. Other studies have addressed the routing problem in a stochastic framework, considering both time-dependent and non-time-dependent models. For instance Dijkstra (1959), Frank (1969), and Hayhurst & Shier (1991) worked on non-deterministic, non-time-dependent shortest path problem and Hall (1986), Fu and Rilett (1998), and Hooks & Mahmassani (2000) worked on non-deterministic, time-dependent shortest path (minimum time) problem. In our approach we assume that with today's sensor and information technology it will soon become possible to have accurate traffic flow information on any segment of the transportation network with virtually zero delay. The availability of such information eliminates most of the uncertainties regarding density and traffic flow rate measurements or predictions and justifies the use of deterministic methods for dynamic routing.

2 ROUTE PLANNING: QUASI-STATIC APPROACH

In this section we consider the problem of route planning before the trip begins. It is considered a static problem since the selected route does not change during the trip. The route-planning problem has been extensively studied in the literature. Some of the

relevant criteria affecting route selection are: minimum distance, minimum travel time, minimum fuel consumption, congestion avoidance, safety, and the possibility to keep moving. Also the characteristics of the vehicle and the trip make a difference as to what criteria are considered more important among drivers, e.g. driving a truck vs. driving a private vehicle [Bovy and Stern, 1990]. As trucks are larger, they are limited by certain road characteristics like width, slopes, and angularity. Also, since truck drivers try to achieve on-time delivery, the criterion of "minimum travel time" is considered extremely important among them.

In this study, in order to apply the minimum travel time criterion to the network under consideration we use a variation of Dijkstra's "shortest path" algorithm [Dijkstra, 1959]. The term "shortest path" could mean the shortest geometric path between an origin and a destination point in a connected network, but it can also be generalized to a path that has a total "minimum cost" between the origin and the destination. In the context of our study, unless otherwise indicated, the term "shortest path" means "minimum time" between origin and destination points. In order to plan the "minimum time" route, we use historical data of average traffic speeds at surface streets or freeway segments within the area under study. The average speed in combination with the segment length obtained from the ArcView Geographic Information System (GIS), provides the travel time for the particular segment. Summation of the travel times for all segments of a particular path between origin and destination provides the total travel time, which will be minimized by the shortest path algorithm. The "minimum time" algorithm was developed in C++, and a brief description is provided below.

2.1 Dijkstra's Algorithm

Terminology: A *transportation network* consisting of nodes and links that connect some of these nodes can be represented by a linear graph $G(V, E, L)$, where V is a set of nodes and E is a set of node pairs (i, j), $i, j \in V$ called links. Nodes i and j are endpoints of link (i, j). Each link is associated with a real number $L(i, j)$ called the length of link (i, j). If two nodes m and n are not connected by a link, i.e. link (m, n) does not physically exist in the network, then it is considered to be a link of infinite length. A transportation network is called *connected* if there is a path between every pair of its nodes. The *path* is a sequence of nodes connected by links in one direction so that a movement is feasible from the first node to the last node in the sequence.

Assumption: The link lengths are nonnegative.

The most efficient combinatorial algorithm for finding the shortest directed paths from a given node s to any other node in a network $G(V, E, L)$ with nonnegative link lengths

$$L(i, j) \geq 0 \text{ for all } (i, j) \in E$$

was first given by Dijkstra (1959). The algorithm is based on assigning labels to the nodes. The labels are continuously updated by an iterative procedure. At each stage, the number assigned to each node represents an upper bound on the directed path length from

s to that node. At the end of the procedure, the node label becomes the exact length of a shortest directed path from *s* to that node in question. In static shortest path, instead of length, the travel time between two nodes could be computed as follows:

$$T(i,j)=L(i,j)/Vij$$

Where Vij is the mean speed between the two nodes and assumed to be constant. To proceed, let each node *i* of *G* be assigned a nonnegative real number $l(i)$ called the *label* of *i*. Initially, all the labels are temporary. At each iteration, one of the temporary labels, say $l(j)$ is made permanent. To distinguish a temporary label from a permanent one, we use $l^*(j)$ to indicate that node *j* has received the permanent label $l^*(j)$. The basic steps of the algorithm are as follows:

Step 1: Set $l^*(s)=0$ and $l(i)=T(s, i)$ for $i \neq s$ and $i \in V$, and $T(s, i)=\infty$ for $i \neq s$ and $(s, i) \notin E$.

Step 2. After (k-I) permanent labels have been established, among all the remaining temporary labels $l(i)$, pick

$$l(k) = \min_i \; l(i)$$

Change $l(k)$ to $l^*(k)$. Stop if there is no temporary label left.

Step 3. Update all nodes *I* that still have temporary labels for which $(k, i) \in E$ by

$$l(i) = \min [l(i), l^*(k) + T(k, i)]$$

Return to Step 2.

A proof of Dijkstra's algorithm is provided in [Dantzig et al., 1997].

2.2 Identification of the Shortest Path

Dijkstra's algorithm determines the lengths of the shortest paths from node *s* to all other nodes *i* (i=1, 2, …, n-1) in the network. However, the paths themselves are not found. To proceed, let each node *i* of *G* be assigned a pointer $p(i)$ to the previous node in the path. The pointers are set in the Step 2 of Dijkstra's algorithm in the following way:

$$p(i) = k \qquad \text{for } l(i) = l^*(k) + L(k, i)$$

We then repeat the process for node *k*. In this way, we can backtrack from node *i* to node *s*, and identify the shortest directed path from *s* to *i*.

2.3 Complexity of the Algorithm

The algorithm consists of operations of comparisons and additions. An operation count for step 2, shows that there are (n-2) comparisons in the first iteration; (n-3) comparisons in the second iteration, etc., so that there are a total of

$$(n\text{-}2) + (n\text{-}3) + (n\text{-}4) + \ldots + 2 + 1 = (n\text{-}1)(n\text{-}2)/2$$

comparisons. Likewise, in step 3 there are n-2 additions and the same number of comparisons the first time, n-3 additions and the same number of comparisons the second time, and so forth. Thus, there are (n-1)(n-2)/2 additions and comparisons in Step 3. As a result, the algorithm requires (n-1)(n-2) comparisons and (n-1)(n-2)/2 additions for an n-node network, and therefore its computational complexity is $O(n^2)$.

3 ROUTE GUIDANCE: DYNAMIC APPROACH

In this section we study an improved solution of the static route-planning problem of section 2, by considering the dynamics of trucks and traffic flow and utilizing on line measurements and information. Here we assume that on-line measurements of average traffic speeds throughout the network are available, in addition to past measurements. The on-line measurements are available to a central information point, which could be located at the trucking company's dispatching center. The on-line data can be transmitted to the truck for in-vehicle processing (distributed guidance system) or they can be processed at the central information point (centralized guidance system). In either case, an optimal route, given the specific updated network conditions, will be generated and the truck will update its original route when arriving at the appropriate intersection. Depending on the availability of technology, the trucks themselves may act as probes as well, so that they will report their position and speed back to the processing center, for further and more accurate updates of network conditions. The dynamic route guidance algorithm was also developed in C++, like the static route planning of Section 2. Details of the algorithm are provided below.

3.1 Dynamic Route Guidance Algorithm

The static algorithm finds the shortest directed paths from a given node s to all other nodes in a network $G(V, E, L)$.

The dynamic algorithm recalculates the shortest path from each node that belongs to the identified shortest path toward the known destination point, taking into account the updated information about traffic speed throughout the network. If there are any changes in the traffic speed on any link (i,j) on the shortest path, a new shortest path will be determined.

In the following dynamic shortest path algorithm we have:

$l(i)$: temporary label of node i
$l^*(i)$: permanent label of node i
$T_{ij}(t)$: travel time from node i to node j at time t

$V_{ij}(t)$: mean speed from node i to node j in time t
L_{ij}: the distance between node i and node j (length of link (i, j))
$t(i)$: the instant of time the vehicle reaches node i (as vehicle traverse on the link (k, i))
s: starting point

Algorithm:

Step 1: Set $t(s) = departure\ time$

$T_{ij}(t_{(s)}) = L_{ij}/V_{ij}(t_{(s)})$ $\quad i, j \in V$

$l(i) = t(s) + T_{si}(t_{(s)})$ $\quad for\ i \neq s\ and\ i \in V,\ and\ T_{si}(t_{(s)}) = \infty\ for\ i \neq s\ and\ (s, i) \notin E$

Step 2: After (k-I) permanent labels have already been established, among all the remaining temporary labels $l(i)$, pick

$$l(k) = \min_i\ l(i)$$

Change $l(k)$ to $l^*(k)$. If there is no temporary label left go to step 4.

Step 3: Update all nodes i's temporary labels which $(k, i) \in E$ by

$l(i) = min\ [l(i), l^*(k) + T_{ki}(t_{(s)})]$
Return to Step 2.

Step 4: If $V_{ki}(t(n)) \neq V_{ki}(t(s))$ $\quad (n \in V)$ *then*, s = n, Go to step 1
Otherwise stop if destination node has been reached. If not, repeat step 4.

Identification of the shortest path: The procedure is the same as for the static guidance case. To show how the algorithm works, let's assume that when a truck is in arc (i, j), congestion occurs in a portion of the route downstream of the vehicle. This means that the average speeds in some portions of the network have now changed, and this information has been relayed back to the center. The average speed for a typical arc (k,m) at the current time, denoted by $V_{km}(t(j))$ is different from the speed $V_{km}(t(s))$ for the same arc (k,m) obtained earlier, at time $t(s)$. The model will find the new shortest path by renaming the current node (j) to be the new starting node (s) and executing the algorithm from step 2 with new speed values.

Complexity of the algorithm: As shown earlier, the complexity of the static Dijkstra algorithm is $O(n^2)$. In the dynamic algorithm, the worst case would be if the route has to be reconfigured every time the vehicle reaches a new node. This means that, in the worst case, the static shortest path algorithm must be executed at each node of the network Assuming that the network has n nodes, the complexity of the dynamic shortest path algorithm will be n times of the complexity of the static one, in the worst case scenario, so the complexity of the dynamic algorithm will be $O(n^3)$.

3.2 Modification of Network Representation

In the “shortest path” algorithm described in Section 2, if the objective were to minimize the geometric distance between the origin and destination, then the only information required would be the link lengths. Dijkstra’s algorithm would solve the problem by providing a sequence of network nodes to be followed, and the summation of the link lengths along the optimal route would be the minimum distance from origin to destination.

If, however, the objective criterion is “minimum travel time”, then the required information is the average traffic speed along each link and the link length. In addition, the number of left or right turns along the route must be taken into account, since the turn times for trucks can be quite long, sometimes comparable to the time it takes to travel along a link. Other parameters that can be significant are the number of traffic lights and the time a truck is waiting for the light to turn green. Recently, the development of real-time guidance systems has attracted renewed interest into the subject of accounting for intersection movements and prohibitions [Ziliaskopoulos and Mahmassani, 1996]. The “shortest path” algorithm described in the previous sections, however, does not allow explicitly for intersection movements.

Dijkstra's algorithms, and indeed, all current shortest path algorithms, are based upon the following fundamental observation:

“If the shortest path between nodes *s* and *t* passes through node *k*, then that segment of the path from node *s* to node *k* is also the shortest path to node *k* from node *s*. In addition, the path from node *k* to node *t* is the shortest path between those two nodes.”

If a node (i.e. an intersection) includes turn delays or turn penalties, then these turn penalties are dependent upon not only the approach link of the node, but also the direction of entry and the direction of exit through the node. In terms of cost for the objective function, the delays or penalties are defined as node related costs. The node costs cannot, however, be directly added to link cost function in Dijkstra's algorithm, since the following is true [Bertsekas, 1992]:

Theorem. In a network with turn penalties, the shortest route from node *s* to node *t* through an intermediate node *k* may not include the shortest route from node *s* to node *k*, or from node *k* to node *s*.

This theorem conflicts with the fundamental observation of Dijkstra's algorithm. In other words, the node costs cannot be directly added to the link cost function when Dijkstra’s algorithm is used.

One way of correctly allowing for turn penalties and prohibitions are to expand the representation of intersections. In this case, each intersection is represented by more than one node, depending on the number of possible turns at the particular intersection. A generic intersection representation is shown in Figure 25. Under the “minimum distance” criterion, a single node would represent this intersection. When taking the turn times into account, however, eight extra nodes are included in the intersection representation, in

order to represent turning movements. For example, if a westbound truck makes a turn towards the south, this movement is represented by the link (*h*,*a*). The newly formed links within the intersection are considered to have zero geometric length. They do have, however, a "time cost" associated with them. The time cost can be different for a left or right turn. It can also accommodate a time penalty for crossing the intersection on a straight line, if appropriate (for example link (*b*,*e*) for a northbound truck, waiting at a red light, will have an associated time cost). If a particular turn is prohibited, then the corresponding links are considered non-existent for the algorithm. The modified intersection in Fig. 25, is now represented by 8 nodes and 12 links.

Clearly, as the level of detail increases so does the complexity of the representation in terms of the number of links and nodes. The modified network structure has a much higher number of nodes but now the standard Dijkstra's algorithm can be directly applied, and the optimal solution will include the cost of turns or waiting for a traffic light at an intersection. A very important feature of the proposed movement representation scheme is that it can be applied in conjunction with "higher-dimension" shortest path algorithms, e.g. time- dependent shortest path, stochastic shortest path and k-shortest path algorithms.

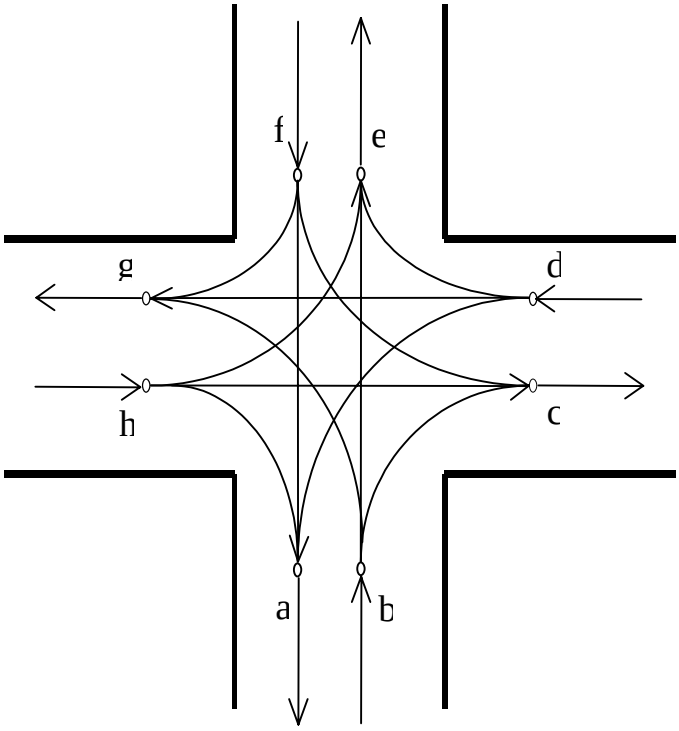

Fig. 25: Modified representation of an intersection

3.3 Truck Turn Characteristics

In this subsection we use the characteristics of trucks studied in part I in order to evaluate the time that it takes to complete turns at intersections. These data are used by the routing algorithm that is developed subsequently.

The following figures describe the truck position and velocity profiles at turns that take place at intersections:

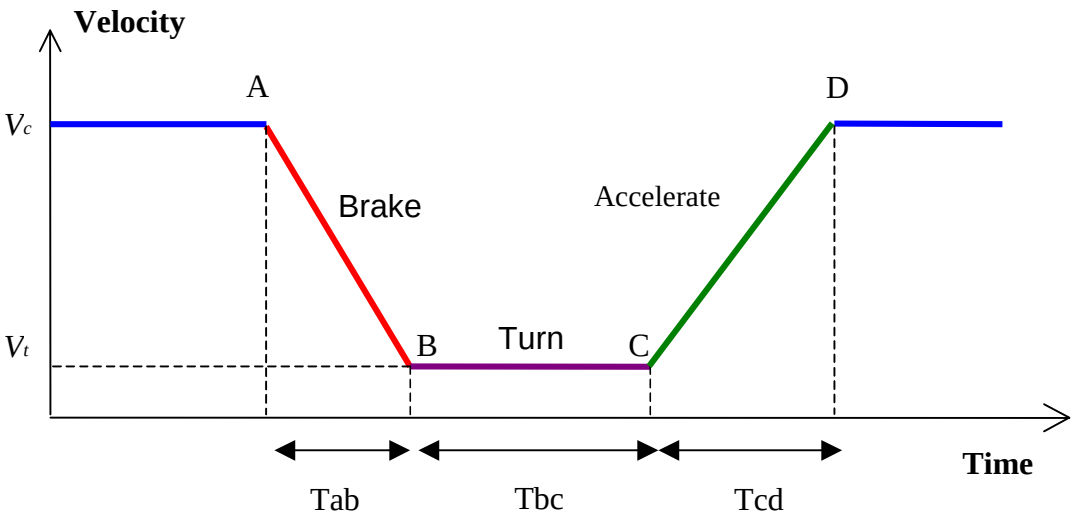

(b)

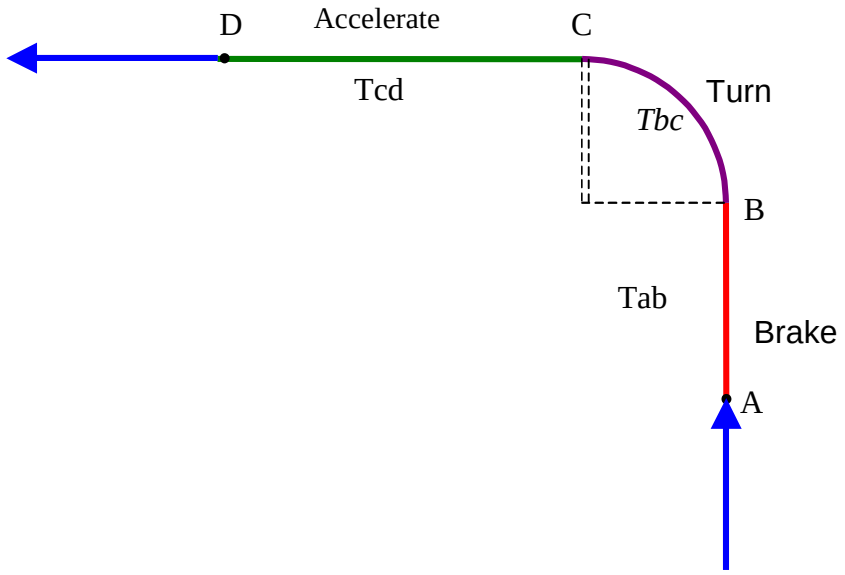

(a)

Fig 26: Truck position and velocity profile at turns

Fig. 26-a shows a typical profile of truck turning at a sharp turn. Let's assume that the truck approaches the point A as indicated by an arrow in Fig. 26-a. At this point, the truck speed is reduced while the vehicle performs the breaking maneuver as shown in Fig. 26-b. *Tab* is the time that breaking maneuver takes place. In other words in this duration of time, the initial constant velocity, *Vc*, will be reduced to the speed in turn, *Vt*, as the truck reaches the point B (Fig. 26-b)

The truck performs the turning maneuver at the constant speed of *Vt* in the time *Tbc* (From point B to C in Fig. 26-a and 26-b). After the turning maneuver is completed (point C in Fig 26-a and Fig 26-b), the vehicle starts increasing its speed from *Vt* to *Vc* with a constant acceleration (point C to D) in *Tcd* seconds. When the truck reaches the speed of Vc, it continues its trip with the same constant velocity as indicated by an arrow in point D in the Fig 26-a.

Using the notation of Fig 26, the total time *T*o of the turning maneuver can be calculated as follows:

$$To = Tab+Tbc+Tcd+Tidle$$

where *Tab* and *Tcd* can be obtained through solving the following equation:

$$Tab= 2Xab/(Vc+Vt) \ : \ Tcd= 2Xcd/(Vc+Vt)$$

where *Xab (Xcd)* is the distance from point A to point B (point C to point D) and *Vc*, *Vt* are the speeds at points A and D and B and C respectively as shown in Figure 26.

Tbc can be also computed using the following formula:

$$Tbc=Xbc/Vt$$

where *Xbc* is the distance from B to C and *Vt* is the speed of vehicle in the turn BC (see Figure 26)

Tidle is the time the truck spends waiting at the traffic light.

The values of turn velocity *Vt* , acceleration and deceleration during the turning maneuver, turning radii (which will determine *Xbc*) etc., that will be used in the simulation runs, are obtained from the truck characteristics studied in Part I of this report.

3.4 Modified Dynamic Routing Algorithm

The dynamic algorithm presented in section 3.1 is modified to include the cost in time at intersections due to traffic light delays and time taken for a truck to complete a particular turn. The nodes now include the possible choices at intersections for different turning directions as well as delays due to traffic lights. In the following dynamic shortest path algorithm we have:

$l(i)$: temporary label of node i
$l^*(i)$: permanent label of node i
$T_{ij}(t)$: travel time from node i to node j at time t
Toij (t) is the time it takes for the truck to turn and/or wait at the traffic light at node i with destination j
$V_{ij}(t)$: mean speed from node i to node j in time t
L_{ij}: the distance between node i and node j (length of link (i, j))
$t(i)$: time the truck arrives at node i
s: starting point

Algorithm:

Step 1: Set $t(s) = departure\ time$

$T_{ij}(t_{(s)}) = L_{ij}/V_{ij}(t_{(s)}) + Toij(t_{(s)})$ $\quad i, j \in V$

$l(i) = t(s) + T_{si}(t_{(s)})$ $\quad$ *for* $i \neq s$ *and* $i \in V$, *and* $T_{si}(t_{(s)}) = \infty$ *for* $i \neq s$ *and* $(s, i) \notin E$

Step 2: After (k-I) permanent labels have been established, among all the remaining temporary labels $l(i)$, pick

$$l(k) = \min_i l(i)$$

Change $l(k)$ to $l^*(k)$. If there is no temporary label left go to step 4.

Step 3: Update all nodes i's temporary labels which $(k, i) \in E$ by

$l(i) = min\ [l(i), l^*(k) + T_{ki}(t_{(s)})]$
Return to Step 2.

Step 4: If $V_{ki}(t(n)) \neq V_{ki}(t(s))$ $\quad (n \in V)$ *then* s = n, Go to step 1
Otherwise stop if destination node has been reached and if not, repeat step 4.

4 CASE STUDY

Several researchers have studied the truck travel patterns in the Los Angeles (LA) region, especially the dependence of these travel patterns on the locations of the major trip generators – manufacturers, warehouses, the ports, and rail yards – as well as on locations of existing trucking terminals [Hall and Lin, 1991, Banerjee et al. 1999]. Of special interest are areas with high concentration of manufacturers and warehouses, such as the area in Los Angeles City Central. This area is in the proximity of the Ports of Los Angeles and Long Beach; Union Pacific's Long Beach intermodal terminal 20 miles south of downtown (ICTF); and the Santa Fe, and Union Pacific intermodal terminals in the vicinity of the downtown.

The recent study by the City of L.A. [Banerjee et al. 1999]) analyzed truck movement and access problems in urban industrial districts. The focus of the study was the geographical area in Central L.A. City East, at the northern end of the Alameda corridor, with a high concentration of trucks and a history of congestion and delay problems. The area includes the major rail intermodal terminals near Downtown LA, LA Intermodal Center, East LA and Hobart rail yards.

After discussions with the city of L.A., this area was chosen as a case study for the current METRANS project. The static and dynamic algorithms described in Sections 2 and 3, were modified and applied to this area as a case study. The first step was to establish a transportation network within the selected area. The transportation network consists of the truck routes within the area under study. It is represented by a set of *54 nodes*, and *83 links*. A link connects two nodes and a node is the intersection of two or more links. Links may be either directed, in which case they specify the direction of movement, or undirected. In this network representation, an intersection is represented by a single node, and each approach by one undirected link. The established transportation network with the node numbers and the corresponding links is shown in Figure 27.

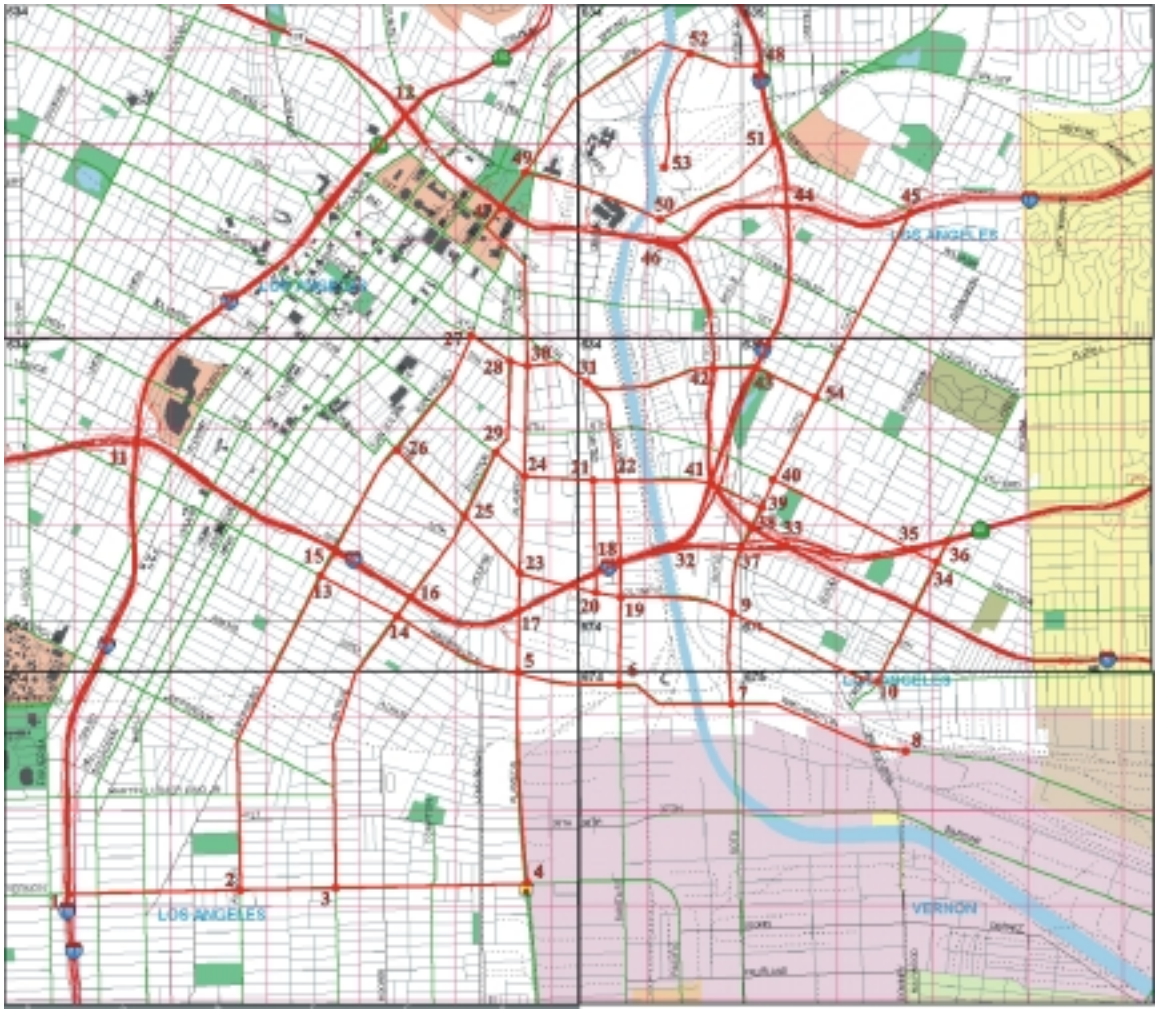

Fig. 27. Truck route network used for the case study: Central L.A. City East

This network has been modified to account for additional links due to different turning possibilities at intersections and delays at traffic lights. The result was the introduction of additional nodes as shown in Figure 28.

Fig. 28: The traffic network with modifications to account for intersection movements

5 SIMULATIONS

The algorithms presented in sections 2 and 3, for route planning and dynamic route guidance are applied to the network of Figure 28, and tested in simulation under different traffic conditions.

In each simulation, an origin (O) and a destination point (D) are defined, for an individual truck's trip. Origin and destination addresses are located on a digitized map and their positions stored as latitude and longitude coordinates. This is done using the address geocoding abilities of ArcView GIS. Since traffic conditions vary with the time of the day, each simulation run is using two different sets of average speeds: *off-peak speeds and peak hour speeds*. For a given origin / destination (O/D) pair, five simulation runs are performed:

(a) *Shortest geometric distance route*. This is the baseline route for each O/D pair, and it is obtained by applying the algorithm using the link lengths as the associated cost. The shortest distance route is denoted by (I) in the simulation figures.
(b) *Static route planning for off-peak conditions*. Dijkstra's algorithm is applied to the established network, including penalties for intersection turns. The (static) minimum time route is denoted by (II) in the simulation figures.
(c) *Dynamic route guidance for off-peak conditions*. The initial route in this case is the same as the one obtained in part (b). As the trip progresses, however, updated information about traffic conditions becomes available. The algorithm is continuously recalculating the optimal path, and informs the drivers of any changes in the original route. The (dynamic) minimum time route is denoted by (III) in the simulation figures.
(d) *Static route guidance for peak conditions.* This is the same as part (b), with different network traffic conditions. The obtained route is denoted again by (II).
(e) *Dynamic route guidance for peak conditions.* This is the same as part (c), with different network traffic conditions. The obtained route is denoted again by (III) in the simulation figures.

The software calculates the optimal route in each case, and it provides driving directions in plain English, so that the dispatcher or driver can follow the route easily.

All the O/D pairs are chosen based on the study of the "Goods Movement Improvement Program, Phase I" (prepared by City of Los Angeles Department of Transportation, LADOT). Average speeds are based on the SCAG study: "SCAG Region Transportation Performance Indicators Technical Report " (97 RTP), and on the 98 RTP Technical Appendix – Freight Component.

	Freeways	Surface streets
Off-peak speeds	45 mph	25 mph
Peak speeds	12 mph	10 mph

5.1 Simulation Experiment 1

In this experiment *node 1 is chosen as the origin*. This is the intersection of I-110 and Vernon St., the most SW point of the network, with a lot of cargo from the ports traveling through. *Node 31 is chosen as the destination*, at Santa Fe Ave. & 4th St. this is a large truck trip generating facility – "Mixed Warehouse District" with 60 docks. The shortest distance route, the static and dynamic route algorithms are applied. The results generated are the following:

a) Shortest distance route: 1-2-3-14-16-25-29-28-30-31 (4.93 miles)

b) Static route planning for off-peak conditions (minimum travel time route): 1-11-15-16-17-18-22-31 (728 seconds).
   Driving directions generated by the software:
   1. Start going north on I-110
   2. Merge onto I-10 E.
   3. Go straight (on I-10)
   4. Take the Santa Fe exit towards 7th St.
   5. Go straight towards 4th St.

c) Dynamic route guidance for off-peak conditions. The initial optimal route is the same as in part (b): 1-11-15-16-17-18-22-31. During the trip, however, information becomes available about delays on I-10 between nodes 17, and 18 and they propagate back to the network. The algorithm recalculates the optimal route: 1-11-15-26-27-28-30-31 (795 seconds). The two routes diverge from node 15 on.
   Driving directions generated by the software:
   1. Start going north on I-110
   2. Merge onto I-10 E.
   3. Take the San Pedro St. exit towards 9th St.
   4. Go straight on San Pedro St. towards 4th St.
   5. Turn right onto 4th St.
   6. Go straight, pass Central Ave.
   7. Go straight, pass Alameda St.
   8. Go straight towards Santa Fe Ave.

d) Static route planning for peak conditions (minimum travel time route): 1-2-3-14-16-25-29-28-30-31 (1900 seconds)

e) Dynamic route guidance for peak conditions. Initial route is 1-2-3-14-16-25-29-28-30-31, same as in part (d). Due to updated information about delays on Central Ave. between nodes 14 and 16, the recalculated route is: 1-2-3-4-5-17-18-22-31 (2063 seconds). The two routes diverge from node 3 on.

It is noted that the route produced by the algorithm in off-peak condition consists of freeway segments (part b), whereas the route during peak hours uses surface streets (d). Figure 29 shows the static (II) and dynamic (III) minimum time optimal routes, superimposed on the network map.

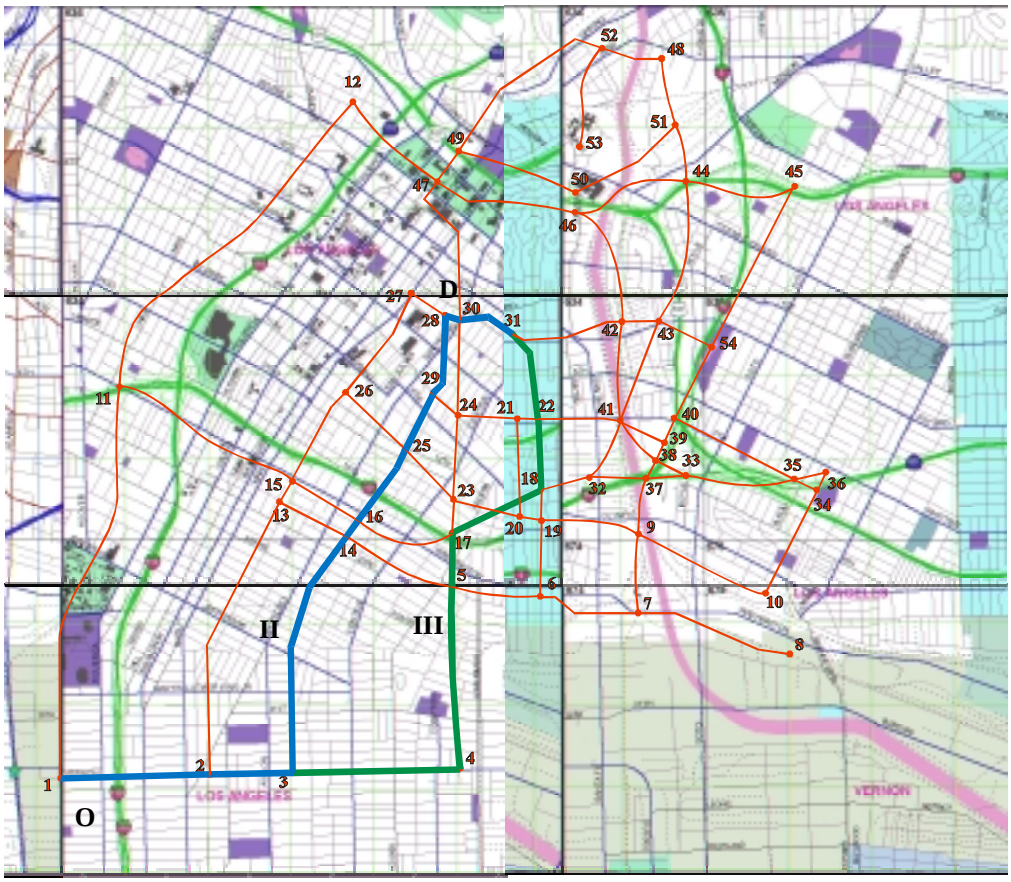

Fig. 29: Simulation experiment 1. Static(II) and Dynamic(III) routes in peak traffic conditions

5.2 Simulation Experiment 2

The *origin is node 49* (Union Station), and the *destination is node 8* (Hobart rail yard)

a) Shortest distance route: 49-47-30-31-22-18-19-9-7-8 (4.4 miles)

b) Static route planning for off-peak conditions (minimum travel time route): 49-47-46-42-41-38-37-9-7-8 (692 seconds).

c) Dynamic route guidance for off-peak conditions. The initial optimal route is the same as in part (b): 49-47-46-42-41-38-37-9-7-8. During the trip information becomes available about delays on I-5 (freeway ramp) between nodes 41 and 38, which propagate back to node 42. Recalculated optimal route: 49-47-46-42-43-54-40-39-38-37-9-7-8 (865 seconds), diverging from the initial route from node 42 on.

d) Static route planning for peak conditions (minimum travel time route): 49-47-46-42-41-38-37-9-7-8 (1614 seconds).

e) Dynamic route guidance for peak conditions. Initial route is 49-47-46-42-41-38-37-9-7-8, same as in part (d). Due to updated information about delays on I-5 between nodes 41 and 38, the recalculated route is: 49-47-46-42-43-54-40-39-38-37-9-7-8 (1838 seconds). The two routes diverge from node 42 on.

In this simulation experiment, static and dynamic routes are the same for peak and off-peak traffic conditions, however the duration of travel is different. Although the shortest geometric distance route includes only surface streets (part a), the minimum time routes (static and dynamic) partially include freeways. This is due to the time cost for turns and for waiting at traffic lights. Figure 30 shows the static (II) and dynamic (III) minimum time routes for peak conditions.

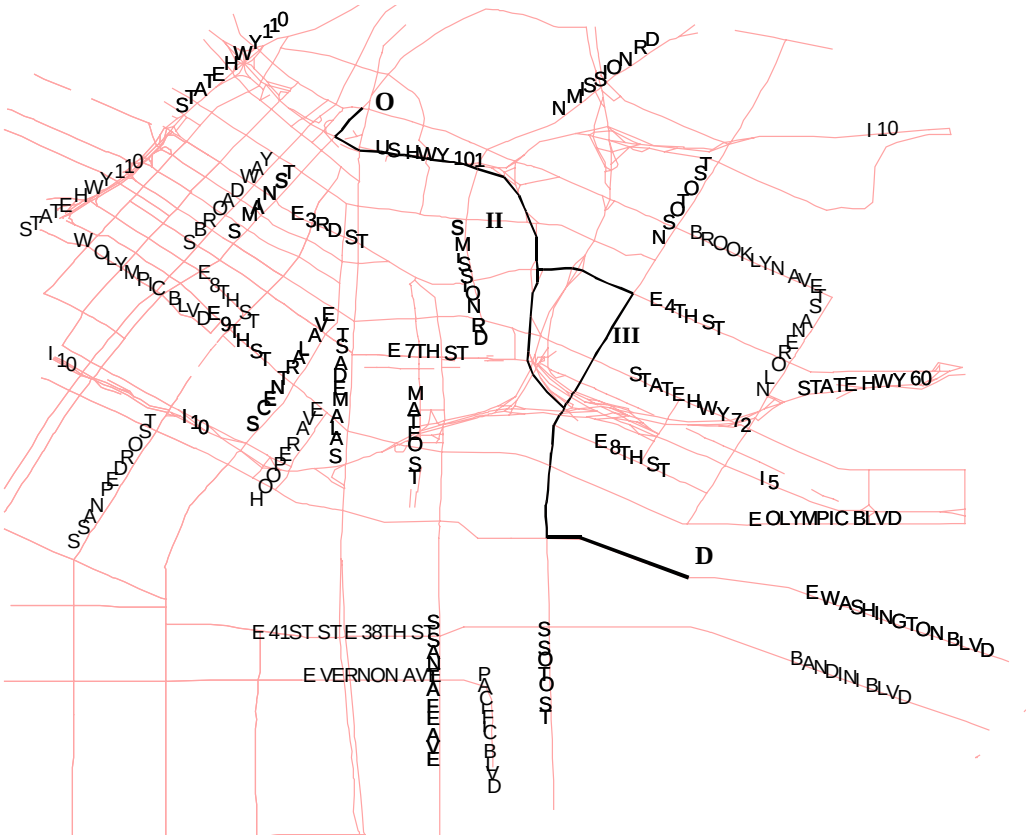

Fig. 30: Simulation experiment 2. Static minimum time route (II) and Dynamic minimum time route (III) for peak and off-peak conditions

5.3 Simulation Experiment 3

The *origin is node 8* (Hobart rail yard), and the *destination is node 26* (San Pedro St & 9th St.). This is a large truck trip generating facility – "City Produce Market".

a) Shortest distance route: 8-7-9-19-20-23-25-26 (3.32 miles)

b) Static route planning for off-peak conditions (minimum travel time route): 8-7-9-19-20-23-25-26 (615 seconds).

c) Dynamic route guidance for off-peak conditions. The initial optimal route is the same as in part (b): 8-7-9-19-20-23-25-26. During the trip, information becomes available about delays on 9th street, between nodes 23 and 25, which propagate back to node 20. Recalculated optimal route: 8-7-9-19-18-17-16-15-26 (1146 seconds), diverging from the initial route from node 19 on.

d) Static route planning for peak conditions (minimum travel time route): 8-7-9-19-20-23-25-26 (1300 seconds).

e) Dynamic route guidance for peak conditions. Initial route 8-7-9-19-20-23-25-26, same as in part (d). Due to updated information about delays on 9th Street, between nodes 23 and 25, the recalculated route is: 8-7-9-19-18-17-16-15-26 (1644 seconds). The two routes diverge from node 19 on.

In this simulation experiment, static and dynamic minimum time routes are the same for peak and off-peak conditions, however the duration of travel is different. Also, the shortest geometric distance route is the same as the minimum time route (Fig. 31).

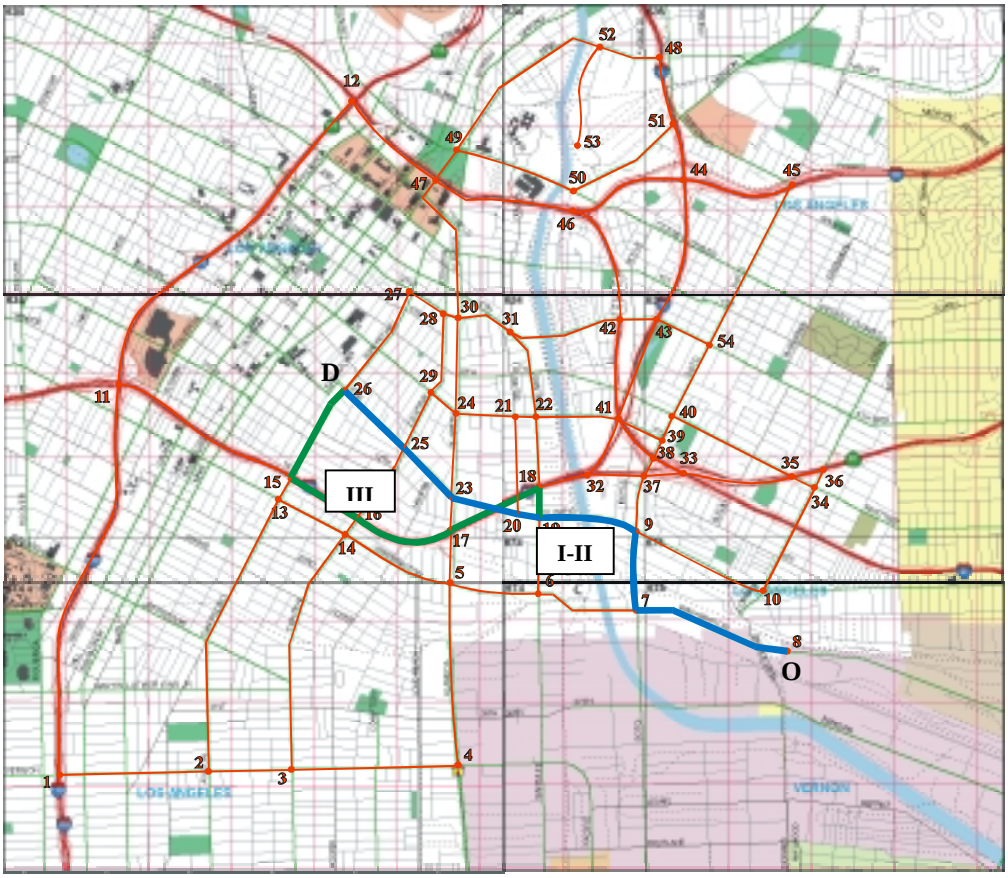

Fig. 31: Simulation experiment 3. Shortest geometric distance & Static route(I-II) ; Dynamic minimum time route (III) in peak and off-peak conditions

5.4 Simulation Experiment 4

The *origin is node 4*, at Alameda St. & Vernon St., which is part of Alameda corridor. The *destination is node 53* (LA Intermodal Center).

a) Shortest distance route: 4 -5-17-23-24-30-47-49-52-53 (5.14 miles)

b) Static route planning for off-peak conditions (minimum travel time route): 4-5-17-18-32-41-43-44-51-48-52-53 (843 seconds).

c) Dynamic route guidance for off-peak conditions. The initial optimal route is the same as in part (b): 4-5-17-18-32-41-43-44-51-48-52-53. During the trip, information becomes available about delays on I-10 (freeway ramp), between nodes 18 and 32, which propagate back to node 17. Recalculated optimal route: 4-5-17-23-24-30-47-49-52-53 (861 seconds), diverging from the initial route from node 17 on.

d) Static route planning for peak conditions (minimum travel time route): 4-5-17-23-24-30-47-49-52-53 (1953 seconds).

e) Dynamic route guidance for peak conditions. Initial route 4-5-17-23-24-30-47-49-52-53, same as in part (d). Due to updated information about delays on Alameda St, between nodes 30 and 47, the recalculated route is: 4-5-17-18-32-41-43-44-51-48-52-53 (2094 seconds). The two routes diverge from node 17 on.

In this simulation experiment, the static off-peak route uses freeways while the static peak route uses surface streets. The static minimum time route for peak conditions is the same as the minimum geometric distance route.

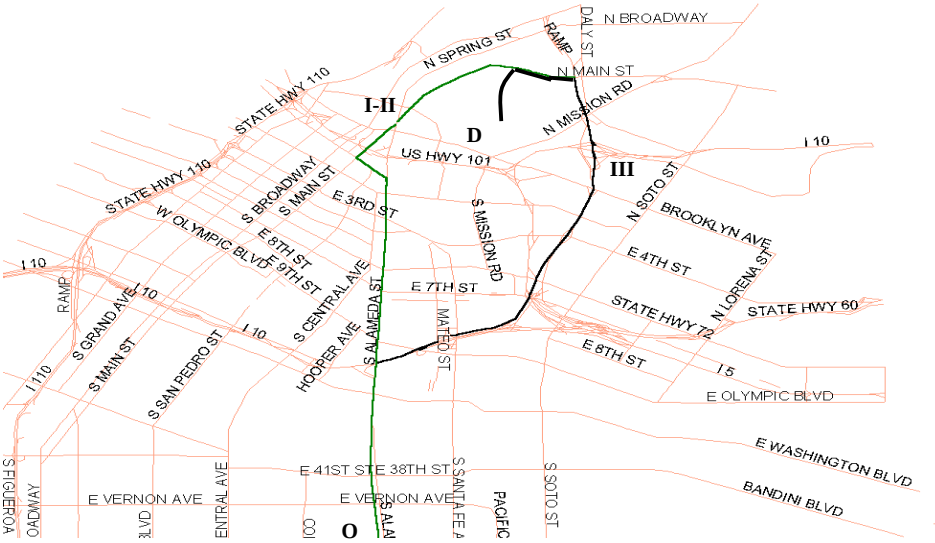

Fig. 32: Simulation experiment 4. Shortest geometric distance & Static route(I-II) ; Dynamic minimum time route (III)

5.5 Simulation Experiment 5

The *origin is node 1*, at I-110 & Vernon St. This is the same origin point as in experiment 1, the most SW point of the network, with a lot of cargo from the ports traveling through. The *destination is node 53* (LA Intermodal Center).

a) Shortest distance route: 1-2-3-14-16-25-29-28-30-47-49-52-53 (6.92 miles).

b) Static route planning for off-peak conditions (minimum travel time route): 1-11-12-47-49-52-53 (880 seconds).

c) Dynamic route guidance for off-peak conditions. The initial optimal route is the same as in part (b): 1-11-12-47-49-52-53. During the trip, information becomes available about delays on I-110, between nodes 12 and 47. Recalculated optimal route: 1-11-15-16-17-18-32-41-43-44-51-48-52-53 (1050 seconds), diverging from the initial route from node 11 on.

d) Static route planning for peak conditions (minimum travel time route): 1-11-12-47-49-52-53 (2415 seconds).

e) Dynamic route guidance for peak conditions. Initial 1-11-12-47-49-52-53, same as in part (d). Due to updated information about delays on I-110, between nodes 12 and 47, the recalculated route is: 1-11-15-26-27-28-30-47-49-52-53 (2779 seconds). The two routes diverge from node 11 on.

In this simulation experiment, the shortest geometric route uses surface streets while the static off-peak route uses freeways. The static minimum time route for peak conditions is the same as the static minimum time route for off-peak conditions, with different travel times.

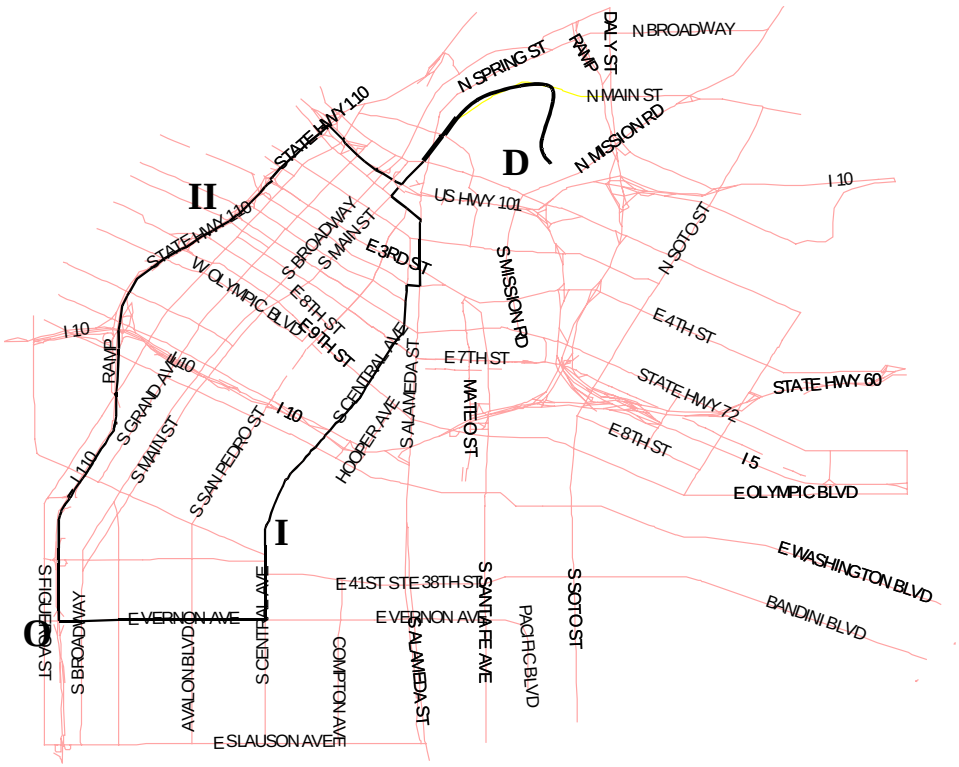

Fig. 33: Simulation experiment 5. Shortest geometric distance route(I) and Static minimum time route (II) during peak and off-peak conditions

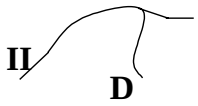

III

O

Fig. 34: Simulation experiment 5. Static route (II) and Dynamic minimum time route (III) during off-peak conditions

5.6 Comparison of Shortest Distances, Static and Dynamic Routing Algorithms

In this section we compare the three algorithms (shortest distance, static and dynamic routing) for two different cases: (1) When there is no change in traffic conditions throughout the truck's trip and (2) When unpredictable traffic delays take place in the network during the truck's trip. The results of simulation 5 were chosen to illustrate the comparison. The results of simulation 5 are summarized as follows:

Shortest distance route: 1-2-3-14-16-25-29-28-30-47-49-52-53(6.92 miles)
Static route off-peak conditions (minimum travel time route): 1-11-12-47-49-52-53 (880 sec)
Dynamic route off peak conditions (congestion on 12-47): 1-11-15-16-17-18-32-41-43-44-51-48-52-53(1050 sec)
Static route peak conditions (minimum travel time route): 1-11-12-47-49-52-53 (2415 sec)
Dynamic route peak conditions (congestion on 12-47): 1-11-15-26-27-28-30-47-49-52-53 (2779 sec)

Case 1: No change in traffic conditions during the trip

In this case we assume that the traffic conditions remain the same throughout the trip. Here the results of the dynamic route algorithm are the same as of the static one. The shortest geometric distance criterion gives the longest travel time, since the shortest route consists mostly of surface street segments, where the average speed is lower than on the freeways. The results of experiment 5 for this case are presented in Table 7.

Table 7: Summary of Example 5 in the Static Conditions Case

Algorithm	Traffic Cond.	Distance (miles)	Travel time (seconds)
Shortest geometric distance	Off-peak	6.92	1263
Static planning (min time)	Off-peak	7.34	880
Dynamic guidance (min time)	Off-peak	7.34	880
Shortest geometric distance	Peak	6.92	2690
Static planning (min time)	Peak	7.34	2415
Dynamic guidance (min time)	Peak	7.34	2415

Results of this type could be used to examine the trade-off between shortest distance and shortest time routes. For example, if other considerations are taken into account, such as cost of fuel, then the additional savings in time by taking the shortest time route may not justify the extra fuel cost, and the shortest distance route may be preferable. Consequently our methodology and results could be used by trucking companies and truck drivers to help them analyze this trade-off and make better routing decisions.

Case 2: Unpredictable changes in traffic conditions during the trip

In this case we assume that an unpredictable traffic delay takes place. The dynamic algorithm is continuously updating the optimal route and informs the driver of any changes in the original route. The shortest distance and static algorithm can not utilize traffic information dynamically and as a result the travel time along these routes will increase with the congestion delay.

Consider the network in example 5 in off-peak conditions. Initially the static and dynamic routes are the same. The algorithm generates the same path for the dynamic route until congestion delay greater than 170 seconds takes place in the route. In this case the dynamic routing algorithm switches to a different route in order to avoid the delay and minimize travel time. As the delay increases, the travel time for the static route increases. Fig 35 and Fig 36 show the effect of delays along the static algorithm route relative to the dynamic route that bypasses these delays.

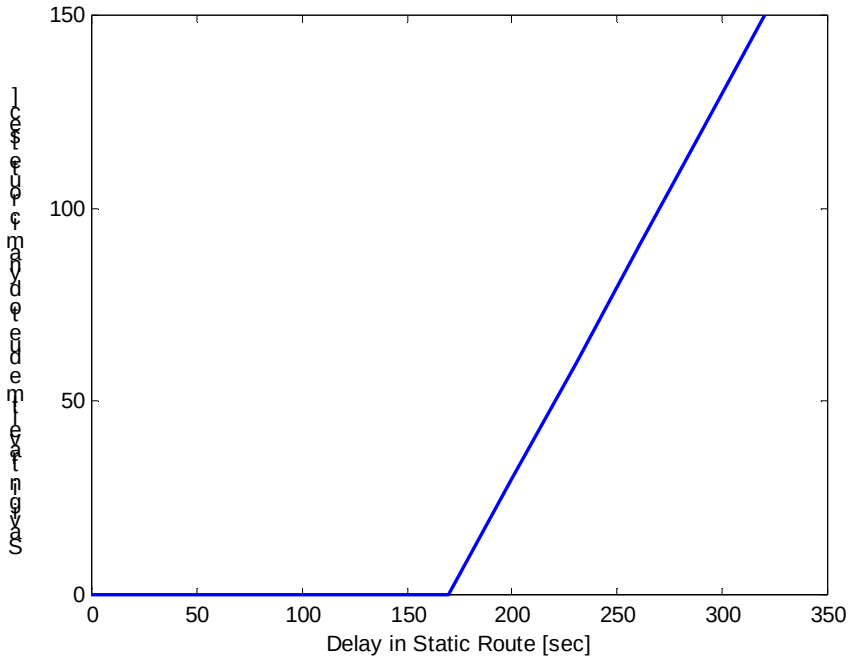

Fig.35: Saving in travel time, using dynamic route for example 5 off-peak conditions, vs. the amount of Delay generated in Static route

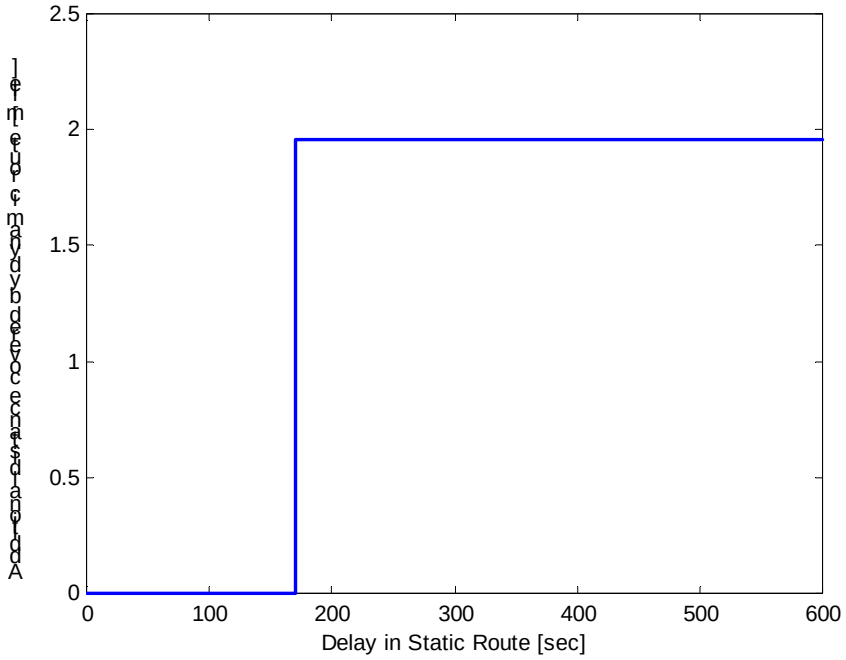

Fig.36: Additional distance covered in dynamic route for example 5 off-peak conditions, vs. the amount of Delay generated in Static route

The results shown in Fig. 35 and Fig. 36 could be used to understand the trade-off between savings in travel time and in travel miles.

Similar results can be generated for the shortest distance algorithm.

6 Conclusions and Recommendations

In part II of this report, we used algorithms for finding the “shortest” route in a complex transportation network. The methodologies used are based on Dijkstra’s algorithm and include the shortest geometric distance, shortest time based on static conditions with no updating along the route (“static route planning”) and shortest time based on continuous updates of information about traffic conditions along the route (“dynamic route guidance”). We assume that the availability of sensors and information technologies makes it possible to have on line information regarding traffic conditions on the network and transmit that information to all relevant parties. This assumption eliminates uncertainties and allows the use of deterministic routing algorithms that are easy to implement. The developed routing algorithms are applied to a specific traffic network in the metropolitan Los Angeles area, which includes the Central Los Angeles City East. Our study demonstrates that significant reduction in travel time can be obtained by using today’s available technologies and the proposed routing algorithms.

Implementation

In part I of this report we show via analysis and demonstrate via simulations the effects of trucks on traffic flow both on the microscopic and macroscopic level. The results compare well with those based on empirical studies. Consequently they can be used with confidence to predict phenomena that are not covered by empirical studies. Our results reinforce the suggestions of traffic engineers to dedicate lanes for trucks only, or to restrict trucks from certain routes and highways where possible. While the dedication of special lanes for trucks only is not possible in general due to the low truck volume relative to passenger vehicle volume, there are places where dedicating lanes just for trucks may be possible. The 710 freeway serving the Port of Long Beach is one example where the volume of trucks is relatively high. We believe that the tools and results developed in this project could be used to examine the effects of dedicating such lanes to trucks and calculating at which truck volume relative to passenger car volume such dedicated lanes will be beneficial to all vehicles involved.

The results of part II of this study are significant for implementation by trucking companies. The proposed routing algorithms could be used to route trucks through any complex transportation networks in order to reduce travel time. The technologies required for implementation of these algorithms are currently available. The use of these technologies results in the elimination of uncertainties regarding traffic flow characteristics, which are important for route selection. Consequently the development and implementation of deterministic dynamic routing algorithms that are reliable and easy to implement is possible as demonstrated in this study. The use of these technologies in the near future will depend on cost issues that have not been considered in this study.

References

Banerjee, F., Okazaki, J., Rifkin, A.D., Bok, S.L., Grawe, C., Mermelstein, S. (1999) "Improving Truck Movement in Urban Industrial Districts*" City of Los Angeles Department of Transportation.*

Batz, T. M. (1991) "The Utilization of Real-Time Traffic Information by the Trucking Industry." *IEEE Transactions on Vehicular Technology* 40/1, 64-67.

Boardman, B.S. (1997) "Real-Time Routing of Shipments Considering Transfer Costs and Shipment Characteristics" *Ph.D. Theses. University of Arkansas*.

Bovy, P. H. L. and Stern, E. (1990) "Route Choice: Wayfinding in Transport Networks" *Kluwer Academic Publishers. Dodrecht/Boston/London.*

Boyce, D.E. (1988) "Route Guidance Systems for Improving Urban Travel and Location Choices." *Transportation Research-A* 22/4, 275-281.

Bose, A., Ioannou, P. (1999) "Analysis of Traffic Flow with Mixed Manual and Semi-Automated Vehicles" *Submitted to the IEEE Transactions on Intelligent Transportation Systems*

Camm, J.D., Chorman, T.E., Dill, F.A., Evans, J.R., Sweeney, D.J., Wegryn, G.W. (1997) "Blending OR/MS, Judgement, and GIS: Restructuring P&G's supply chain." *Interfaces* 27/1, 128-142.

Cassidy M. J., M. J.(1999) "Traffic Flow and Capacity", *Handbook of Transportation Science*, Ed. Randolph Hall, 151-186, Kluwer Academic Publishers.

Chandler, P. E., Herman, R., and Montroll, E. W.,(1958)"Traffic Dynamics: Studies in Car Following", *Operations Research,* vol. 6, 165-184

Cohen, S.(1991) "Traffic Variables", *Encyclopaedia of Traffic Flow,* Ed. M. Papageorgiou. 139-143.

Cook, K. L.; Halsey E. (1969), "The Shortest Route Through a Network with Time-Dependent intermodal Transit Times", *Journal of Mathematical Analysis and Applications 14, 492-498*

Crainic, T. G., Laporte, G. (1997) "Planning Models for Freight Transportation." *European Journal of Operational Research* 97, 409-438.

Dantzig, G.B, Thapa, M.N. (1997) "*Linear Programming 1: Introduction*" *Springer-Verlag*.

Dijkstra, E.W. (1959) "Note on Two Problems in Connection with Graphs." *Numerical Mathematics* 1, 269-271.

Dongjoo, P. (1998) *Multiple Path Based Vehicle Routing in Dynamic and Stochastic Transportation Networks.* Ph.D. Theses. Texas A&M University.

Dreyfus, S.E. (1969) "An Appraisal of Some Shortest-Path Algorithms." *Operations Research* 17 395-412.

Enke K.(1979) "Possibilities for improving safety within the driver vehicle environment control loop." *7th international technical conference on experimental safety vehicles. Washington D.C., National Highway Traffic Safety Administration.*

Fancher , P. et al. (1994) "Predictive Analysis of the Performance of a Headway Control System for Heavy Commercial Vehicles*" Supplement to Vehicle System Dynamics – Vol. 23*

Fancher ,P ; Gillespie , T. D.,(1997) "Synthesis of Highway Practice 241- Truck Operating Characteristics", *Transportation Research Board, National Academy Press, Washington, D.C.*

Frank H., (1969) "Shortest Paths in Probabilistic Graphs", *Operations Research, vol. 17*

Fu, L. and L. R. Rilett (1998), "Expected Shortest Paths in Dynamic and Stochastic Traffic Networks", *Transportation Research B, Vol. 32, No. 7, 499-516*.

Gans, N., van Ryzin, G. (1999) "Dynamic Vehicle Dispatching: Optimal Heavy Traffic Performance and Practical Insights." *Operations Research* 47/5, 675-692.

Hall, R.W., Intihar, C. (1997) "Commercial Vehicle Operations: Government Interfaces and Intelligent Transportation Systems*", California PATH Research Report UCB-ITS-PRR-97-12.*

Hall, R.W., Lin, W. H. (1991) "Less-Than-Truckload Trucking in Los Angeles: Congestion Relief Through Terminal Siting." *Transportation Research Record* 1320, 47-57.

Hall, R. W. (1986), "The Fastest Path through a Network with Random Time-Dependent Travel Times", *Transportation Science 20,182-188*

Hayhurst, K.; Shhier, D. (1991), "A Factoring Approach for the Stochastic Shortest Path Problem", *Journal of Operations Research, 329-334*

Ho, F.S., Ioannou, P., (1996) "Traffic Flow Modelling and Control Using Artificial Neural Networks." *IEEE Control Systems Magazine* 16/5. 16-27.

Ioannou, P. (1997) "Automated Highway Systems" *Plenum.*

Ioannou, P. et al. (1996) "Inter vehicle Spacing – User's Manual*" CATT Report University of Southern California*

ITE Tech. Council Committee (1992) "Geometrical Design and Operational Considerations for Trucks" *Institute of Transportation Eng. Washington , DC*

Jula H., et al., (2000) "Collision Avoidance Analysis for lane changing and Merging", *IEEE Transaction on Vehicular Technology*, Vol. 49, No. 6, pp. 2295-2308.

Kanaris, A., Ioannou, P.; Ho Fu-Sheng (1996), "Spacing and Capacity Evaluations for different AHS Concepts" *CATT – Report – University of Southern California*

Kaufman, D.E., Smith, R.L. (1993) "Fastest Paths in Time-Dependent Networks for IVHS Applications." *IVHS Journal* 1/1, 1-11.

Lawler E. L. (1976), "Combinatorial Optimization: Networks and Matroids", *New York : Holt, Rinehart and Winston, c1976*

Lighthill, M.J., and Whitham, G. B (1955) "On Kinematic Waves: A Theory of Traffic Flow on Long Crowded Roads", *Proc. of the Royal Society of London,* A229, No. 1178, pp.317-345

List, G.F., Turnquist, M.A. (1995) "A GIS Based Approach for Estimating Truck Flow Patterns in Urban Settings." *Journal of Advanced Transportation* 29/3, 281-298.

Meyer, Mohaddes Associates, Inc. (1996) *Gateway Cities Trucking Study*. Gateway Cities Council of Governments Southeast Los Angeles County.

Miller, H.J., Wu, Y.H., Hung, M.C. (1999) "GIS-Based Dynamic Traffic Congestion Modelling to Support Time-Critical Logistics." Proceedings of the Hawaii International Conference on System Science.

Miller-Hooks E., Mahmassani, H. (2000), "Least Expected Time Paths in stochastic Time-Varying Transportation Networks", *Transportation Science, 34, 198-215*

Newcomb,T.P.(1977) "*Basic Principles* in Braking of Road Vehicles" I Mech. E. Conf. Publ. 1976 – The Institution of Mech. Eng. – London and N.Y.

Ng, L., Wessels, R.L., Do, D., Mannering, F., Barfield, W. (1995) "Statistical Analysis of Commercial Driver and Dispatcher Requirements for Advanced Traveller Information Systems." *Transportation Research-C* 3/6, 353-369.

Osegueda, R., Garcia-Diaz, A., Ashur, S., Melchor, O., Chang, S-H., Carrasco, C., Kuyumcu, A. (1999) "GIS-Based Network Routing Procedures for Overweight and Oversized Vehicles." *Journal of Transportation Engineering* 125/4, 324-331.

Pipes, L. A. (1953) "An Operational Analysis of Traffic Dynamics", *J. of Applied Physics*, vol.24, 271-281

Qiang, L. (1997) "Simulation-Based Dynamic Traffic System: GIS Approach*" Ph.D. Theses. Department of Civil and Environment Engineering. University of Kanzas.*

Regan, A.C., Golob, T.F. (2000) "Trucking Industry Perceptions of Congestion Problems and Potential Solutions in Maritime Intermodal Operations in California." *Transportation Research-A.* In Press.

Shiller, Z., Sundar, S. (1998) "Emergency Lane-Change Maneuvers of Autonomous Vehicles" *Journal of Dynamic Systems, Measurements and Control-ASME*-Vol. 120-pp.37-44

Shladover S.E., et al.(1991), "Automatic Vehicle Control Development in the PATH Program," *IEEE Transaction of Vehicular Technology*, Vol. 40, PP. 114-130,.

Taoka,G.T.(1989)"Brake Reaction Times of Unalerted Drivers*" .ITE Journal* –March 1989,19-21

Transportation Research Board (1998), "Highway Capacity manual, Special Report 209", *National Research Council, Washington D.C.*

Van Winsum, W. (1993) "Selection of Routes in Route navigation Systems In A.M. Parkes, S. Franzen (eds.) Driving Future Vehicles" *Taylor & Francis Inc.*

Weigel, D., Cao, B. (1999) "Applying GIS and OR Techniques to Solve Sears Technician-Dispatching and Home-Delivery Problems." *Interfaces* 29/1, 112-130.

Zhan, F. B. and Noon, C. E. (1998) "Shortest Path Algorithms: An Evaluation Using Real Road Networks." *Transportation Science* 32/1, 65-73.

Ziliaskopoulos, A., Mahmassani, H. (1996) “A Note on Least Time Path Computation Considering Delays and Prohibitions for Intersection Movements.” *Transportation Research-B* 30/5, 359-367.

.